Title
A TWO-DIMENSIONAL DIFFUSION LIMITED SYSTEM FOR CELL GROWTH

Author
Hlatky, L.

Publication Date
1985-11-01

Lawrence Berkeley Laboratory
UNIVERSITY OF CALIFORNIA

A TWO-DIMENSIONAL DIFFUSION LIMITED SYSTEM FOR CELL GROWTH

L. Hlatky
(Ph.D. Thesis)

November 1985

Donner Laboratory
Biology & Medicine Division

Prepared for the U.S. Department of Energy under Contract DE-AC03-76SF00098

DISCLAIMER

A TWO-DIMENSIONAL DIFFUSION LIMITED SYSTEM FOR CELL GROWTH

Lynn Hlatky

Ph.D. Thesis

Lawrence Berkeley Laboratory
University of California
Berkeley, California 94720

November 1985

This work was supported by the U.S. Department of Energy under
Contract Number DE-AC03-76SF00098.

A TWO-DIMENSIONAL DIFFUSION LIMITED SYSTEM FOR CELL GROWTH

Lynn Hlatky

ABSTRACT

A new cell system, which we call the "sandwich" system, was developed to supplement multicellular spheroids as tumor analogues. Sandwiches preserve many of the crucial features of spheroids, but have important differences that allow new experimental approaches to questions of diffusion, cell cycle effects and radiation resistance in tumors. In this thesis we discuss the method for setting up sandwiches; we characterize the system theoretically and experimentally; and we report on its response to x-ray irradiation.

In the sandwich system cells are grown in a narrow gap between two glass slides. Because of this sandwiching of cells, nutrients and waste products can move into or out of the local environment of the cells only by diffusing through the narrow gap between the slides. Due to the competition between diffusion and consumption of the cells, self-created gradients of nutrients and metabolic products are set up. The result is a layer of cells which is, roughly speaking, like a living spheroid cross section. Sandwiches show the standard spheroid pattern of a cycling outer region, a slowly proliferating middle region and a necrotic center. However, sandwiches differ from spheroids in several important ways. Unlike the cells of the spheroid, cells in all regions of the sandwich are visible. Therefore, the relative sizes of the regions and their time-dependent growth can be monitored visually without the fixation and sectioning necessary in spheroids. In sandwiches there is no three-dimensional cell to cell contact. The oxygen and nutrient gradients can be "turned off" at any time without disrupting the spatial arrangement of the cells by removing the top slide of the assembly, and subsequently turned back on if desired. Removal of the top slide also provides access to all the cells, including those near the necrotic center, of the sandwich. The cells can then be removed for analysis outside the sandwich system.

DNA labelling studies and flow cytometry along with visual observation were used to characterize the system. Our experiments show that the observed cell necrosis, similar to that found in spheroids, is due to diffusion limitations. The results observed are consistent with the idea that oxygen deprivation stops cell cycling and, when extreme and prolonged, leads to necrosis. The possibility that substances other than oxygen are involved is not excluded by the data.

We also report on the x-ray irradiation of 9L sandwiches immediately following removal of the top slide. In this way we determine if cells near the necrotic center of a sandwich have a different radiation sensitivity than those near the nutrient supply apart from hypoxia considerations. Our data indicates that cells near the necrotic region have an increased radioresistance, even when they are irradiated in the presence of oxygen. This increased resistance can not be explained by hypoxia, three-dimensional cell contact, or even two-dimensional cell confluence. One explanation may be that the cells are out of replication cycle, due to nutrient deprivation, and therefore have more time to repair their damage before reaching some critical event in the cell cycle. This idea of nutrient deprivation inducing a state where there is more time to repair was checked by irradiating nutrient deprived 9L cells grown in monolayer. These cells also show an increased radiation resistance as compared to monolayer cells grown in complete medium.

TABLE OF CONTENTS

INTRODUCTION

I. TUMORS

A. Salient Features of Tumor Growth

Cells in different parts of a tumor usually have different properties owing, *inter alia,* to limitations on the diffusion rates for nutrients and metabolic products. In poorly vascularized tumors, such diffusion gradients often result in necrotic regions, in regions of hypoxic cells, in a reduced fraction of proliferating cells as the tumor ages and thus a progressive slowing of the overall growth rate, and in various other phenomena which affect the tumor's radiation response.

B. Diffusion Limitations

As early as 1942, Caspersson and Santesson suggested three possible causes for the development of necrosis in tumors. These were lack of oxygen, lack of glucose, or the toxic effect of high concentrations of lactic acid. The first of these, lack of oxygen, gained popularity as the favored hypothesis.

The work of Thomlinson and Gray (1955) supported the hypothesis that tumor necrosis might be a direct result of oxygen deprivation, in view of the agreement between the location of necrosis seen in tumor histological sections with the calculated oxygen diffusion distance, both being about 150μm.

A similar value for the oxygen diffusion length was estimated by Goldacre & Sylven (1962), who considered diffusion of a dye into the necrotic region of tumors and by Rajewsky (1965), who demonstrated that the depth of *in vitro* labelling of tumors with [^{3}H]TdR depends on the oxygen tension of the medium. With the subsequent improvements in microelectrodes, regions of low oxygen tension have been directly measured in various types of tumors (Vaupel *et al.*, 1973).

In 1968, Tannock did an extensive study of the spatial relation of the necrotic regions in mouse mammary tumors to the tumor vascularization; his findings were also consistent with

the anoxia hypothesis. Tannock further suggested that limitations in oxygen may be what causes viable cells to leave the cycling population thereby reducing the growth fraction to less than unity.

Several successful models of tumor growth have been proposed based on the idea that the rate of growth of a tumor is limited by nutrient diffusion (Burton, 1966; Greenspan, 1972).

C. Cell Cycle Distributions

Histological sections of labelled tumors examined autoradiographly exhibit varying regions of high and low labelling. Using [^{3}H]TdR to label the tumors *in vivo*, a clear relationship has been found between the labelling index and the proximity of cells to a blood vessel. The labelling index drops with distance from the blood vessel. For the case of mouse mammary tumors, cells in contact with the vessel had a labelling index of $\sim$74%, while those farthest from the vessel exhibited a labelling index of only 30% (Tannock, 1968). Oxygen deprivation has been suggested as a possible cause for this drop in the labelling index. Similarly, for tissue specimens labelled *in vitro* the labelling index has been correlated with the oxygen tension (Fabrikant, Wisseman & Vitak, 1969; Rajewsky, 1965).

As cells located at too great a distance from the blood vessel leave the cycling population they accumulate in the G_1 stage of the cell cycle (Harris, Meyskens & Patt, 1970). The increasing proportion of cells in the G_1 state means a decreasing tumor growth fraction. This loss of cells from the proliferating pool is a major reason for the slow-down in the growth rate observed in tumors (Steel, 1977). An increase in the cell cycle time of the cycling cells would also slow down the tumor growth rate, but such an increase seems to be the exception rather than the rule for solid tumors (Tannock, 1968; Frindel, Malaise, Alpen & Tubiana, 1967).

A certain amount of cell migration in tumors has been observed by following cells labelled with a single injection of [^{3}H]TdR as they moved from regions of contact with the blood vessel to those regions furthest from the vessel (Tannock, 1968).

D. Radiation Response

There are two points of particular interest to us concerning the radiation response of tumors. The first is that tumors are more radioresistant if irradiated *in vivo* than if irradiated in as single cells *in vitro* (Steel, 1977; Rockwell & Kallman, 1973; Dawson *et al.*, 1973; Hill *et al.*, 1979; Wallen *et al.*, 1980). This phenomenon is consistant with the so called "contact effect" for spheroids (Durand & Sutherland, 1972), whereby growth of cells in three-dimensional contact confers an extra radioresistance. Once the tumor is dissociated into single cells the cells soon lose this capacity for extra resistance. The second point is that many tumors contain radiobiologically hypoxic cells (Rockwell & Kallman 1973). Hypoxic cells are found in regions too far from the vascularization to get an adequate oxygen supply. These cells are often adjacent to necrotic regions. The presence of hypoxic cells in tumors limits the effectiveness of radiotherapy. This limitation is due to the reoxygenation and subsequent regrowth of the tumor from the core of hypoxic cells that were preferentially resistant to the radiation due to their anoxic state.

II. SPHEROIDS

A. An In-Vitro Tumor Model

Spheroids are spherically shaped non-clonal aggregates of cells grown in suspension culture (Yuhas, 1977). The spheroid system was developed by Sutherland, McCredie & Inch (1971) as an *in vitro* tumor model. In many ways spheroid growth mimics tumor growth, and spheroids have a histological pattern very similar to that of the poorly vascularized tumors mentioned earlier. Like tumors, spheroids are subject to three-dimensional cell-to-cell contact and to diffusion limitations. Due to some combination of these factors, spheroids develop features similar to those of poorly vascularized tumors. When intermediate in size they begin to exhibit dynamic properties such as: a progressive slowing of the growth rate (Durand, 1976), and a decreasing growth fraction accompanied by a shifting of interior cells into a G_1 state. Upon reaching a critical size spheroids develop a necrotic center. Like tumors, many spheroids show a radiation resistant tail on survival curves, and an overall resistance when irradiated in the associated rather than the dissociated state. Recently spheroids of mixed cell

types have also shown a degree of differentiation.

B. Diffusion

In spheroids the geometry is simpler than in tumors and the external environment is controllable; thus a more detailed check of the oxygen diffusion hypothesis became possible. By the examination of cross sections of fixed spheroids good evidence was found to support the idea that oxygen deprivation plays a major role in the onset of necrosis in spheroids (Carlsson 1979; Franko & Sutherland 1979a). But some of this same work suggests that in addition to oxygen some other factor (nutrient or toxin) may be important. It is also of interest to note that the literature (Koch *et al.*, 1973; Balin *et al.*, 1976; Born *et al.*, 1976; Franko & Sutherland, 1978). is ambiguous when it comes to the question, can hypoxia alone cause massive cell necrosis?

More recently work has been done to see what role glucose deprivation plays in the onset of necrosis (Mueller-Klieser *et al.*, 1983). An attempt to model the glucose distribution of the 9L spheroid, with respect to the viable and necrotic zones, was published by Li in 1982.

C. Cell Kinetics

The cell cycle distribution of spheroids closely resembles that of the poorly vascularized tumors we discussed earlier. Small spheroids exhibit a different cell cycle distribution than do large spheroids. In small spheroids most of the cells are cycling, resulting in nearly exponential growth. As the size of the spheroid increases more and more cells leave the cycling population thereby reducing the growth fraction. This reduction in the growth fraction is a major determinant in slowing down the spheroid growth rate (Durand, 1976; Yuhas & Li, 1978), just as was seen for the case of tumors. When the spheroid reaches a large size there are essentially three populations of cells: a population of actively cycling cells which is found close to the nutrient source; a population composed of primarily noncycling cells which is further from the nutrient source; and a population of necrotic cells furthest from the source of nutrients. The cells in this second, noncycling, population are mostly in the G_1 stage of the cell cycle (Allison *et al.*, 1983). A cross section taken from a large labelled spheroid reveals

these populations (Durand, 1976).

D. Radiation Response

There are several features of the radiation response of spheroids that are characteristic of most spheroid systems, although it has been shown (Durand, 1980) that details of the radiation response vary depending on the cell line and the actual growth conditions. Spheroids of many cell lines show a radioresistant tail on their survival curves (Sutherland & Durand, 1976; Franko & Sutherland, 1979b; Dertinger & Hulser, 1981). This is presumably due to the region of hypoxic cells surrounding the central necrotic core. Sutherland & Durand (1973) made the first estimate of the proportion of hypoxic cells in a spheroid on the basis of this radiation resistant tail. Attempts have also been made to isolate cells from different regions of the spheroid in order to check the regional radiation response with individual cells rather than trying to infer it from survival curves done on "whole" spheroids. One method used for separating cells in spheroids is that of sequential trypsinization (Freyer & Sutherland,1980; Giesbrecht, Wilson & Hill, 1981). More recently the method of fluorescence-activated cell sorting, which utilizes the diffusion gradients of spheroids, has been used (Durand, 1982). Durand's data (1983) suggests that, when hypoxia considerations are eliminated, the inner spheroid cells are slightly more sensitive to radiation than the outer cells.

Apart from the radioresistant hypoxic cells found in spheroids, most cell lines grown as spheroids show an increased radioresistance over cells of the same cell line grown in monolayer. This resistance is primarily seen in the shoulder region of the survival curve (Durand & Sutherland, 1973), but for some cell lines (e.g. 9L) the slope is modified without significant change in the extrapolation number (Rodriguez & Alpen, 1981). The effect is analogous to the increased resistance seen for solid tumors when irradiated in the associated rather than dissociated state. The hypothesis was put forth (Durand & Sutherland, 1972) that the increased radioresistance may stem from the three-dimensional intercellular contact during spheroid growth. Populations of cells grown as spheroids, but irradiated after spheroid dissociation show that this elevated resistance decays with time after dissociation. Although many

investigators have confirmed the existence of the so called "contact effect", no explanation of this phenomenon has yet emerged (Olive & Durand, 1985; Dertinger, Hinz & Jacobs, 1982; Rasey, 1983).

III. SANDWICHES

This thesis describes a new, two-dimensional, diffusion limited system for cell growth, which we have come to call the "sandwich" system. Sandwiches were developed to supplement spheroids as models for tumor growth. Sandwiches preserve many of the crucial features of spheroids, but have important differences that allow new experimental approaches to questions of diffusion, cell cycle effects and radiation resistance in tumors.

The sandwich system is, roughly speaking, a living cross section of a spheroid in which all the cells are visible. Sandwiches show the standard spheroid pattern of a cycling outer region, a slowly proliferating middle region and a necrotic center. The relative sizes of these regions and their time-dependent growth can be monitored visually without the fixation and sectioning necessary in spheroids. The geometry is such that the width of these regions in the sandwich is greatly enlarged compared to those in spheroids. This enlargement proves useful in many cases, for example when looking at the gradient of labelled cells.

Another difference from spheroids, beside the visibility and amplification of the three regions, is that one has access to the cells in all regions of the sandwich. One advantage of this access is that the radiation response of cells in the different individual regions of the sandwich can be studied in a clean and easy way. That is, one can irradiate the whole sandwich and then separate out the subpopulations for individual plating. Exploiting this advantage of the sandwich system, x-ray studies were performed to determine if cells near the necrotic center of a sandwich have a different radiation sensitivity than those near the nutrient supply. Our data suggests that cells near the necrotic region have an increased radioresistance, even apart from considerations of hypoxia. This is possibly explained by the fact that these cells are out of cycle and therefore may have more time to repair their damage before reaching some critical event in the cell cycle.

In the sandwiches diffusion processes are in effect one dimensional. We can therefore use the diffusion equation in one dimension with an appropriate consumption term to analyse our data, rather than using the three-dimensional equation appropriate to spheroids. This change in dimensionality provides a way to evaluate the current hypothesis that oxygen diffusion limitations cause necrosis. Previous work apart, the results of our sandwich experiments do strongly indicate that necrosis is due to the competition between diffusion of some nutrient or toxin (e.g. oxygen, glucose, lactic acid,...) and the consumption or production of this substance by the cells. Our results are consistent with oxygen being this substance, although they do not exclude the possibility of other substances or of cooperative effects.

As was seen in the case of tumors and spheroids, labelling studies on sandwiches indicate that cells away from the nutrient source progressively go out of cycle. Flow cytometry indicates that these cells pile up in the G_1 state.

This thesis characterizes the sandwich system and points out how aspects of its growth parallel those of spheroids and tumors. We also point out the ways in which sandwiches differ from spheroids. These differences offer possibilities for new approaches to old questions of tumor growth and tumor response to radiation and chemicals. With further experiments it may be possible to make the sandwich system yield a large amount of information about diffusion, consumption, the radiation response of hypoxic cells, and the actions of various substances in circumstances similar to those in a three-dimensional vascularized tumor system. Indeed the sandwich system should be applicable in many other situations where diffusion is the critical factor.

MATERIALS AND METHODS

I. CELL CULTURE

9L cells from a rat gliosarcoma were used for all experiments. The 9L cell line originated from an N-nitrosomethylurea induced tumor in a CD Fisher rat. The tumor was then developed as an *in vivo-in vitro* tumor model. One characteristic of this cell line is that the variation of radiosensitivity with age is anomalously flat, apart from the sensitive periods of G_2 and mitosis (Kimler & Henderson, 1982; Keng & Wheeler, 1980). Our laboratory obtained the initial stock culture from D. Deen (Brain Tumor Research Center, Univ. of California School of Medicine, San Francisco, Ca.).

All cultures were grown in Eagles MEM with Earle's salts (Gibco), supplemented with glutamine, 11% newborn calf serum (Gibco), and 4% fetal calf serum (Irvine Scientific); bicarbonate buffer was added. The oxygen concentration of the air-saturated medium at 37°C was measured to be 0.28±0.04mM using an oxygen electrode (Transidyne General). Cultures were incubated at 37°C in a humidified atmosphere of 5% CO_2 in air.

Stock monolayer cultures were grown in 75 cm^2 flasks (Corning) and were passaged twice a week. These stock cultures were renewed from early-passage frozen stock after~40 passages *in vitro*. The cells used for the radiation studies discussed in this text are from a different frozen stock than those used for the rest of the experiments discussed. As a consequence, the length of the cell cycle is different and a growth curve for each case is given in the Results section with the appropriate experiments.

The glucose and lactic acid concentrations of the medium were measured spectrophotometrically using enzymatic assays (Sigma). The pH was measured by standard electrometric methods. These same measurements were always made on the medium of monolayer or sandwich cultures at the time of experiments in order to characterize the medium.

II. SANDWICH SYSTEM

In the sandwich system, cells are grown in a narrow gap between two glass microscope slides. The cells are grown in a monolayer on the bottom slide. Medium fills the narrow gap between the slides and separates the cells from the top slide. Because of this sandwiching of cells, all nutrients and waste products can move into or out of the local environment of the cells only by diffusing through the narrow gap between the slides. Cells for both the sandwiches and the control monolayers were seeded at 1×10^5 cells/slide, on 1×3 inch, 1mm thick autoclaved glass slides (Corning). The slides had been placed in 3.5×3.5 inch integrid petri dishes (Falcon), three slides per dish. When pipetting cells onto the slides an effort was made to distribute the cells uniformly. The slides were then covered with 10 ml of complete medium and incubated at 37°C and 5% CO_2 for 24 hr. After the 24 hr incubation the slides were removed and placed in new dishes. Two slides per dish were held in place using specially designed plexiglass holders and 14 ml of fresh medium was added to cover the slides. This amount was more than enough to insure that the gap between slides was completely filled in all cases.

At this point the density of cells on the slide is still low, $\approx8\times10^3$cells/cm^2. One fourth of the slides were taken to be control monolayer slides and were placed back in the incubator. From the remaining slides, sandwich cultures were formed by the addition of a top slide resting on spacers, sandwiching the cells between slides (Fig. 1). Spacers were of several types: glass, teflon or wire and ranged in vertical spacing dimension from 60 μm to 300 μm. This range of spacer sizes proved an appropriate one for the 9L cell line. The top slides were autoclaved and treated with prosil-28 (PCR Research Chemicals Inc.), an organosilane nonstick surface coating. This facilitated easy removal of the top slide for the labelling studies and the x-ray studies. Spacers and prosil treated slides were tested and found to be nontoxic to our monolayer cultures. The time of transferring the slides and adding top slides to the sandwiches is referred to as the "setup" time. The age of sandwiches and of their respective control monolayers is measured relative to that.

Note on the Fig. 1 that the x direction is parallel to the short dimension of the slide, the y direction is parallel to the long dimension, and the z direction is perpendicular to the slide. The gap height Z_g is considerably larger than the height of a single cell layer.

Since medium fills the gap above the cells, one might presume that the culture would resemble a monolayer culture rather than a spheroid. However, it is clear that the total transport of oxygen, nutrients, or metabolites in the x direction is much less than it would be if Z_g were as large as the height of medium above a typical monolayer. Thus, as discussed in more detail below, the competition between diffusion and consumption in a sandwich is quite similar to the same competition in a spheroid. As long as the gap height is small compared to the thickness X_b of the viable border the main effect of having medium in the gap above the cells is merely to decrease the effective number of consuming cells per unit volume, which in turn decreases the steepness of the diffusion gradients.

III. MEASUREMENTS OF THE VIABLE CELL BORDERS IN SANDWICHES

Integrid Petri dishes containing sandwich cultures were placed directly on the microscope stage and regions of dead cells were identified visually. This visual identification technique for live and dead cells was verified by Trypan blue exclusion. The width of the viable border, X_b, was measured *in situ*, using a Zeiss inverted phase microscope. These measurements were made at least once a day in order to observe the time dependence of the border. At the time of measurement it was also noted whether the cells were normal looking or had an altered morphology; regions of elongated cells were recorded.

IV. THYMIDINE LABELLING INDEX (TLI) IN SANDWICHES

Sandwich cultures grown at several gap sizes, Z_g, were pulse-labelled at various times after setup along with unsandwiched glass slide monolayers. Cells were labelled with the cover slide removed, and then were fixed and developed in place on the slides. Thus labelling was done without disturbing the crucial spatial arrangement of the cells; of course the microenvironment of the cells changes once the glass top is removed. In this way we were able to get a labelling index for each region of the slide, reflecting the influence of pre-existing media

gradients. We used short labelling times; therefore it is unlikely that the cell cycle distribution alters during the labelling process.

Sandwich and monolayer slide cultures were labelled using [^{3}H]TdR (6.7 Ci/mmol, New England Nuclear) at a concentration of 0.5μCi/ml. At the time of labelling the media was drawn off the cultures and aliquots from each culture were sampled for the pH and the nutrient state, as discussed under cell culture methods above. The top slide was removed from the sandwich cultures without disturbing the cells attached to the bottom slide. Prewarmed conditioned media containing the label was added to the dishes holding the slides. After preliminary studies, 15 min of 37°C incubation was chosen as the labelling time. Slides were then washed three times in PBS, fixed in 3:1 ethanol:acetic acid, rinsed three times in 70% ethanol, air dried and dipped in Kodak NTB-3 emulsion. After four days of exposure the slides were: developed (Kodak D-19); fixed; and stained with hematoxylin.

The labelling index at different x, distances, into the sandwich was obtained by division of the viable border into 500μm strips and a thymidine labelling index (TLI) for each of these strips was determined. This division of the entire viable border into 500μm strips was fine enough in the sense that almost no labelled cells were found in the innermost region and coarse enough that there was a measurable difference between strips. In control monolayers five 500μm strips evenly spaced across the slide were counted. A total of one thousand cells was counted in each strip. A cell was scored as labelled if it had at least ten grains.

V. FLOW CYTOMETRY MEASUREMENTS IN SANDWICHES

In preparation for flow cytometry, cells were removed from the slides. In the case of the control monolayers, cells were trypsinized off the slides and pipetted repeatedly to achieve a single cell suspension. In the case of the sandwich cultures the removal of the cells involved several steps. First, the top slide was removed. Thereupon cells and cell debris from the visually identified necrotic area floated into the medium and could be flushed off the slide. The cells in the viable border, including those with altered morphology, were undisturbed. These remaining cells were then trypsinized off and were pipetted into a single cell suspension.

Once the cells were in a single cell suspension, both control monolayer and sandwich cells were treated following the procedure of Vindelov *et al* (1983) in order to obtain a propidium iodide stained nuclear suspension, as follows. To isolate the nuclei the unfixed cells were digested, using a 10 min treatment in trypsin plus sperminetetrahydrochloride (Sigma) in citrate buffer. The sperminetetrahydrochloride stabilizes the nuclei against disintegration by the trypsin. After this 10 min treatment, trypsin inhibitor plus Ribonuclease (Sigma) in citrate buffer is added; after another 10 min the propidium iodide (Sigma) in citrate buffer is added. The nuclear suspension is then kept in the dark and on ice for at least 30 min. Immediately before flow cytometric analysis the suspension is filtered through a 50μm mesh.

Flow cytometry was performed with a FACS IV (Becton Dickinson) using the 488nm line of an argon laser. 100,000 fluorescent nuclei were collected per histogram. Analysis of the histograms was done using a current version of the Dean & Jett (1974) program. In order to evaluate the change in the cell cycle distribution due to sandwich age, sandwiches and their corresponding control monolayers were analyzed at several different times after setup.

VI. X-RAY EXPERIMENTS

A. Irradiation Procedure

X-ray studies were done on monolayer and 150μm gap sandwich cultures using a 150 kVp Phillips x-ray machine, with 1 mm Al and 0.5 mm Cu filtration. Preliminary experiments were done both at 37°C and at 0°C with no significant change in the results detected between the two temperature conditions. We chose to do the irradiations on ice in order to have easily reproducible temperature conditions, and to slow down repair during the irradiation procedure. The dosimetry was also done on ice. An NBS calibrated Victoreen condenser R-meter was used for the dosimetry. The monolayer flasks and petri dishes containing the sandwich cultures were on a rotating platform 23 cm below the aperture during the irradiation. At this distance there was no measurable variation in the dose rate over the area of interest. The dose rate was ~100 rad/min as measured by the Victoreen. In the case of cells irradiated on glass, there was an additional dose from the glass backscatter; the increase was dose

multiplying and was estimated to be 50% using cell survival as a biological dosimeter. See Fig. 2.

When irradiating on ice, the cells were placed on the ice 5 min prior to irradiation and kept on ice until trypsinization.

Monolayer cultures, both those on glass and plastic, were trypsinized and plated in the standard way following the irradiation. The sandwich cultures were treated in a manner described below, in accordance with the procedure of the particular experiment.

No feeder cells were used in any of the x-ray experiments. For each dose two to three dilutions were seeded, four replicate flasks per dilution. The flasks were incubated at 37°C for at least 11 days. They were then stained with methylene blue, air dried and counted. The criterion for a viable colony was 50 cells.

B. Measuring the Radiosensitivity of Interior Versus Exterior Border Cells

In order to examine the radiation sensitivity of sandwich cells apart from any hypoxia considerations, the top slide was removed just prior to the irradiation. As a result all the cells were oxygenated at the time of irradiation. We looked for differences between the radiation sensitivity of cells in the outer half (by width) of the sandwich border and cells in the inner half. The sensitivity of the entire border population was also measured for comparison.

Cultures were irradiated on ice. The top slide was removed at the same time the petri dish containing the culture was put on ice, i.e. 5 min prior to irradiation. After irradiation, the medium was drawn off and the slides were rinsed with fresh medium in order to flush the slides of dead cells and debris.

At this point, if we were interested in the whole border population rather than separating the border into an exterior half and an interior half, the procedure was as follows: rinse with EBSS-EDTA (Earle's Basic Saline Solution w/o Ca^+ and Mg^+ (Gibco) with .002 g/l EDTA added); trypsinize cells off the slide; pipette into a single cell suspension; and plate. If we wished to look separately at the cells from the exterior half of the border and those from the

interior half, we followed the procedure outlined in Fig. 3. Two replicate sandwiches were used for each dose point, one for the exterior and one for the interior border cells. The cells from that half of the viable border that was not to be collected were scraped off with a spatula and allowed to float into the medium. This separation was done under the dissecting microscope, and the width of the portion being scraped off was measured using the graticule in the microscope ocular. The medium with the floating cells was then drawn off and the slide rinsed with EBSS-EDTA. The only cells remaining on the slide were those in the region of interest. These cells were trypsinized off the slide, pipetted into a single cell suspension and plated.

C. X-Ray Experiments on Unfed Monolayers

The x-ray survival of monolayer cultures, whose medium was never replenished, was followed for ten days. This was done as follows. A large number of monolayer cultures were set up at 1×10^5 cells per $25cm^2$ flask (Falcon), with 5ml of complete medium. Each day, for a period of 10 days in all, a subset of these monolayer cultures was x-rayed. The medium in the flasks was not changed or supplemented prior to the irradiation. The cell number, and the glucose and lactic acid concentration of the medium, were monitored daily. Flow cytometry was also performed on these cultures to follow the progression of cells as the population shifted from a cycling to a noncycling one, due to nutritional deprivation. In addition, a parallel set of studies on unfed monolayers grown on glass slides were also conducted. For these experiments, the cells were set up in the same manner as the sandwich cultures described above but never covered with a top slide.

THEORY

This section discusses some of the theoretical calculations needed to interpret our results. It includes several calculations of diffusion relevant to the sandwich system, including the question of local depletion of the medium at the edge of sandwiches. Convection in sandwiches is also considered.

I. DIFFUSION IN SANDWICHES

It is believed that necrosis in spheroids results from diffusion limitations on some key substance. The substance most often considered is oxygen. Various mathematical models have been used to describe diffusion limitations in spheroids (Burton 1966; Greenspan 1972; Franko & Sutherland 1979a). We shall need sandwich analogues of such models. A basic model of this kind and then some variations will now be presented.

All models that we have compared to the data involve some form of the diffusion equation

$$\partial f/\partial t = D\nabla^2 f - Qn$$

Here f is the concentration of the key substance. D is the diffusion constant, n is the number of cells per unit volume, and Q is a consumption rate, which could depend on f. We first discuss the simplest model of this kind, which will be called the "basic model".

A. An Oxygen Limited Model

In the basic model the key substance is taken to be oxygen; thus $D = 2\times10^{-5}\text{cm}^2/\text{sec}$. There are now four time scales to be considered. The first is the "gap diffusion time" T_g , i.e. the time required for oxygen to diffuse vertically from the top of the gap through the medium down to the cells. $T_g = Z_g^2/D$. For a gap width $Z_g = 60\mu\text{m}$ this gives $T_g \approx 2$ sec. Next is the "border diffusion time" $T_b = X_b^2/D$ required for oxygen to diffuse horizontally from the outside to the necrotic region. For $X_b = 2\times10^3\mu\text{m}$ this gives $T_b \approx$ ½ hr (we give times appropriate for a 60 μm gap width). Third is the "consumption time" T_c during which the cells consume a significant fraction of the oxygen in their own immediate vicinity, $T_c = f/Qn$. For example, if $f = 0.28\text{mM}$, $Q = 10^{-13}\text{mol/cell-hr}$, $n = 10^7/\text{cm}^3$ we get $T_c \approx 1/4$ hr . Note that T_c and T_b

being of the same order of magnitude is consistent with having a measurable oxygen gradient. Finally there is the time for Qn to double due to cell growth and similar processes; we may take this to be approximately the doubling time of our cells $T_d \approx 13$hr.

We now can list a number of assumptions for the basic model. We assume the term involving time derivatives in the diffusion equation above is negligible compared to the term involving space derivatives. Of course $\partial f/\partial t$ cannot be strictly zero. However in our experiments T_d is large compared to the other times of interest. We can thus regard the system as being in an "adiabatically changing steady state" and taking $\partial f/\partial t = 0$ is appropriate.

In the basic model n is taken independent of x and y in the region where n is non-zero. We further take Q to be spatially constant. This assumption is made even for those cells which are viable but, presumably due to low oxygen in their immediate neighborhood, are not cycling. Also f is independent of y; this merely refers to the directly observed absence of significant edge effects (the very ends of the slides were excluded when making measurements). Furthermore, we assume that cells die whenever the oxygen concentration drops to a critical value f_c; interaction terms due, for example, to cooperation between low oxygen and high lactic acid or other substances are neglected in the basic model.

Finally, one needs an assumption about the z dependence of the oxygen concentration. In subsection C below we shall see that if the oxygen concentration in the medium directly above the cells is different from the oxygen concentration in the volume where cells are present the difference can be neglected provided diffusion from the top of the gap to the cells below is very rapid. Specifically one needs $T_g \ll T_b$ and $T_g \ll T_c$. In our case these inequalities hold. Therefore we can assume f to be independent of z and, as the model of subsection C below shows, we may replace n by N/Z_g, where N is the number of cells per unit area (a constant at any one time by the assumptions above). In this sense varying the gap width Z_g merely corresponds to changing the cell density.

Under these assumptions f is a function $f(x)$ of x alone and one must merely solve the ordinary differential equation $f''=k$ where the constant k is (QN/DZ_g) for $0<x<X_b$ and is zero

otherwise. The boundary conditions are the following: at $x=X_b$, $f'=0$; at $x=0$, f has the ambient value $f_a=0.28\pm0.04$mM.

The solution for f thus has the form

$$f=f_c+\tfrac{1}{2}k(x-X_b)^2 \tag{1}$$

in the region $0<x<X_b$ and f is constant in the region where the cells are dead (Fig. 4). Solving Eq. 1 for X_b we get

$$X_b=[2(f_a-f_c)Z_gD/QN]^{1/2} \tag{2}$$

The basic model just described is the one we use to interpret our data. For example we shall vary Z_g to check the proportionality of X_b and $Z_g^{1/2}$. For completeness, later subsections describe how the model is changed when some of its assumptions are modified.

B. Variable Consumption or Density

Suppose, to be more realistic, that the cell growth rate and/or oxygen consumption rate is not spatially constant, but depends on the local environment. Then a modification of the basic model arises in which the term Qn becomes a function of x. We remark that, while Eqs. (1) and (2) then no longer hold, the proportionality of X_b and $Z_g^{1/2}$ is valid under rather general assumptions. In fact, suppose that, as discussed above, the time derivative term in the diffusion equation is negligible ("adiabatic steady-state" assumption). Suppose further that x does not appear explicitly in any of our governing equations and d/dx appears nowhere except in the diffusion equation.("local environment" assumption). Finally, suppose ("initial homogeneity" assumption) that the initial density N at $t=0$ can be regarded as independent of x, i.e. that we can neglect the effects due to a finite x dimension of the slide and are careful to seed uniformly. Then one can rescale *via* $x \longrightarrow x/Z_g^{1/2}$ and all the governing equations of the system remain invariant. Thus the solution will remain invariant, and this implies X_b proportional to $Z_g^{1/2}$. Roughly speaking, if the scaling does leave the equations invariant, cells at a "corresponding place" will always have the same environment, and thus all cells will have the same history.

C. Local Depletions

In the case of spheroids it has been shown that there can be substantial oxygen depletion in the microenvironment surrounding spheroids. It is therefore necessary to examine the local oxygen depletion of the medium just outside the sandwich. Specifically, we shall show that for typical values of the parameters, the oxygen concentration at the edge of the sandwich (i.e. at $x=0$) is at least 90% of the value $f_a=0.28$mM it has at the medium-air interface. Fig. 5 shows the relevant geometry; the arrows indicate the direction of the oxygen flux F (units: *moles* $cm^{-2}sec^{-1}$) caused by the oxygen gradients. In a steady state the flow of oxygen through the surface $x=0$ balances the consumption in the sandwich. Therefore at $x=0$ we have $QNlX_b=FlZ_g=(D\partial f/\partial x)lZ_g$, where l is a dimension in the y direction. Thus $\partial f/\partial x]_{x=0} = QNX_b/DZ_g$. Now on the outside of the sandwich we can assume as an approximation that the flux is radially inward in the region outside the smallest semicircle (of radius $Z_g/2$) shown. For steady state we then have

$$\partial f/\partial r=\gamma/r \tag{3}$$

where γ is determined by $\partial f/\partial r]_{Z_g/2}=QNX_b/D\pi Z_g$. Let R be the average distance from the entrance $x=0$, $z=Z_g/2$ of the sandwich to the medium-air interface. Integrating Eq. 3 gives for the decrease Δf in f: $\Delta f=\gamma\, ln(2R/Z_g)$. Assume, as will be shown to be consistent in a moment, that to zeroth order we can use Eq. 2 with f_c negligible compared to f_a. We now get

$$\Delta f/f\approx(Z_g/\pi X_b)ln(2R/Z_g). \tag{4}$$

Here R is about $0.25cm$ and, since the dependence on R is logarithmic, it need not be specified too precisely. For $Z_g=60\mu$m and X_b the corresponding observed value of about 1300μm Eq. 4 gives $\Delta f/f\approx0.065$. Similarly for $Z_g=150$, $X_b=2000\mu$m we get $\Delta f/f\approx0.08$. Thus at $x=0$ f is within 10% of f_a and our use of Eq. 2 to zeroth order was valid; the fact that $f_c\ll f_a$ will be discussed in detail later in the thesis. Thus our estimates are self consistent and give at most a 10% correction for local depletions just outside the sandwich.

A check on the above calculation is given by the following argument. In the region outside the sandwich the concentration f obeys Laplace's equation. We can introduce elliptical coordinates (μ, θ) centered at $x=0$, $z=Z_g/2$ in the (x,z)*plane* (Morse and Feshbach 1953). Then the line $\mu=0$ in this plane (a "degenerate ellipse") can be identified with the line $x=0$ at the entrance to the sandwich. By separating Laplace's equation in elliptical coordinates one can find a solution for f appropriate to our situation, approximating the air-medium interface as an ellipse. The answer for $\Delta f/f$ comes out the same as in Eq. 4 except that $ln\,2R/Z_g$ is replaced by $ln\,4R/Z_g$ (Morse and Feshbach 1953); because the change is merely in the logarithmic factor our above estimates are not affected significantly.

It would probably be fairly easy to measure the value and the Z_g dependence of Δf in Eq. 4 using oxygen probes. This has not yet been done but should eventually provide a further check on the overall model.

A similar calculation applied to the z gradient of oxygen within the sandwich gives a gradient $\partial f/\partial z \approx NQ/D$ and thus a change in f from the top of the sandwich to the bottom of $\Delta f \approx 2f_a Z_g^2/X_b^2$. This change is negligible except perhaps for the region just next to the necrotic region. Vertical gradients are analyzed from a different point of view in the next subsection.

D. Vertical Diffusion

To show that vertical diffusion (i.e. diffusion in the z direction) can actually be treated as instantaneous, as was done in subsection A above, we shall analyze a generalization of the basic model where the concentration does depend on z and show that this z dependence does not affect the results in a crucial way.

Suppose that for $0 \le z \le Z_1$, where Z_1 represents the height of the cell layer, we have one concentration of oxygen, $f_1(x)$, and that for $Z_1 \le z \le Z_g = Z_1 + Z_2$ we have another, $f_2(x)$ (see Fig. 6). Each one of the functions f_1 and f_2 obeys the diffusion equation, with an extra term that accounts for the flow of oxygen from the upper medium to the cells. We take the diffusion constant D to be the same in both regions (generalizing still further, to the case where the two

diffusion constants are different, is straightforward but will not be discussed here). Thus the equation $d^2f/dx^2=k$ of the basic model above is replaced by the two equations

$$Z_1\, d^2f_1/dx^2 + (1/H)(f_2-f_1) = \alpha \tag{5}$$

$$Z_2\, d^2f_2/dx^2 - (1/H)(f_2-f_1) = 0. \tag{6}$$

Here the constant H has the dimensions of a distance and its order of magnitude is the gap height Z_g. $\alpha=kZ_g$ so $\alpha=QN/D$ for $x<X_b$ and $\alpha=0$ in the necrotic region $x>X_b$. The boundary conditions are that at x = 0 both f_1 and f_2 equal f_a, that necrosis occurs at $x=X_b$ when $f_1=f_c$ and that both f_1 and f_2 remain bounded as x approaches ∞.

Eqs. 5 and 6 can be solved exactly by taking appropriate linear combinations. Adding the equations we find $u''=\alpha$ where u is defined by

$$u=Z_1f_1+Z_2f_2. \tag{7}$$

Solving this differential equation for u with the appropriate boundary conditions gives in the region $x\le X_b$

$$u = (\alpha/2)(x^2-2xX_b) + Z_gf_a. \tag{8}$$

Now define $\Delta=f_2-f_1$. Combining Eqs. 5 and 6 gives

$$\Delta''-\kappa^2\Delta = -\alpha/Z_1 \tag{9}$$

where κ is defined by $\kappa^2=(1/H)[(1/Z_1)+(1/Z_2)]$. Since $\Delta(0)=0$ the solution to Eq. 9 has the form $\Delta = (\alpha/\kappa^2Z_1)(1 - \cosh\kappa x + A\sinh\kappa x)$ in the region $x<X_b$; here A is an integration constant. For $x>X_b$, $\alpha=0$ and only the decaying solution proportional to $e^{-\kappa x}$ is allowed. Insisting that the solutions and their derivatives match at $x=X_b$ gives A and the form we shall need for Δ, namely

$$\Delta = (\alpha/\kappa^2Z_1)(1 - e^{-\kappa x} - e^{-\kappa X_b}\sinh\kappa x). \tag{10}$$

Combining the definition of Δ with Eqs. 7, 8 and 10 now gives

$$f_1 = (k/2)(x^2-2xX_b) + f_a - (Z_2k/Z_1\kappa^2)(1-e^{-\kappa x}-e^{-\kappa X_b}\sinh\kappa x). \tag{11}$$

Now the fact that $f_1 = f_c$ at $x = X_b$ gives us a transcendental equation for X_b, namely

$$f_a - f_c = (k/2)[X_b^2 + HZ_2^2(1 - e^{-\kappa X_b})^2/Z_g]. \tag{12}$$

Using $H \simeq Z_g$ and the numerical values quoted in our discussion of the basic model we find $\kappa X_b \gg 1$ and $HZ_2^2/Z_g \ll X_b^2$. Thus Eq. 12 simplifies to $f_a - f_c = kX_b^2/2$, which is equivalent to Eq. 2. Similarly, the function $f_1(x)$ in Eq. 11 does not differ significantly from $f(x)$ for the basic model. Thus taking into account vertical diffusion gradients changes the basic model only via small correction terms.

E. Substances Other Than Oxygen

There is some evidence (Carlsson, 1979; Franko & Sutherland 1979a; Mueller-Klieser & Sutherland, 1981) that oxygen is not the only substance controlling necrosis in spheroids. We now consider modifications of the basic model in which one other substance plays a critical role, either alone or in combination with oxygen.

Any other substance by itself, whether it is a nutrient like glucose or a toxic metabolite can be substituted for oxygen in the basic model by simple modifications. For the case of a nutrient we need merely make the following changes: (a) use the appropriate diffusion constant D; (b) use the correct consumption rate Q; (c) replace f_a above by the nutrient concentration in the medium outside the sandwich at any one time (we assume this concentration varies slowly compared to the border diffusion rate T_b and consumption rate T_c); (d) and, finally, replace f_c above by the appropriate critical concentration. For example in the case of glucose we find with $D = 6 \times 10^{-6} cm^2$ /sec, $Q = 6 \times 10^{-13}$ mol/cell-hr, $N/Z_g = 10^7$/ml, $f_a \rightarrow 6 \times 10^{-6}$ mol/ml and $f_c \rightarrow 0$ that $X_b = 2000 \mu$m.

A single toxic metabolite is hardly more difficult to handle. The main difference is that the consumption rate Q in the diffusion equation and in Eq. 2 is negative, and k in Eq. 1 is correspondingly negative. Eq. 2 still holds, with the ambient concentration f_a now smaller than the critical toxic concentration f_c. Because Eqs. 1 and 2 still hold there are many calculations and heuristic arguments where we can substitute "excess" (of a toxin) for "lack" (of a

nutrient) without changing anything essential except for a sign.

One can also consider a situation where there are two critical nutrients, e.g. oxygen and glucose, with cell death resulting if either drops below its own critical concentration. Assuming our adiabatic steady state hypothesis such models give nothing new at any one instant: instantaneously, one of the two nutrients is the critical one. The only novel feature of such models is that in general there may be a specific time at which the formerly critical nutrient becomes non-critical and vice-versa. This slight gain in generality is paid for by an increase in adjustable parameters which the experiments are presently too limited to determine.

II. CONVECTION IN SANDWICHES

To estimate whether convection plays an important role in sandwiches we make two order of magnitude calculations. First, if, within the incubator, the sandwich is slightly tilted and there are some temperature gradients there may be a steady convection current. Our estimates indicate that in order to get a significant effect one needs a tilt and/or temperature gradient much larger than normally occurs. Second, we estimate how much the medium between slides moves when a sandwich is handled. We shall see that, even if the handling is quite careful, normal hand motions set up enough convection to move the medium between the slides distances of the order of the width of the viable rim.

In the first estimate, we assume there is a temperature difference ΔT between two opposite edges of the sandwich slides, accompanied by a height difference H (Fig. 7). We check whether currents are set up which move at speeds comparable in order of magnitude with the diffusion rates.

For a fluid with coefficient of viscosity η between glass plates a distance Z_g apart the average speed v of viscous flow for a pressure difference ΔP in distance L is of order

$$v = \Delta P Z_g^{\,2}/4\eta L \tag{13}$$

If ΔP corresponds to a temperature difference ΔT accompanied by a height difference H for a fluid with a thermal coefficient of expansion β, we have $\Delta P = \Delta\rho g H \Delta T = \beta\rho g H \Delta T$. The

condition that convection effects be small compared to diffusion effects is $v \ll X_b / T_b = D / X_b$, i.e. $(Z_g)^2 X_b << 4\eta DL / \rho g H \beta \Delta T$. The values for water are $\beta = 2 \times 10^{-4} K^{-1}$, $\rho = 1$ g cm $^{-3}$, $g = 10^3$ cm sec $^{-2}$, $\eta = 10^{-4}$ dyne cm $^{-2}$ sec , $D = 2 \times 10^{-5}$ cm ^{2} sec $^{-1}$. For a tilt of 2° or less, L/H is at least 30. Finally, temperature differences of more than 10^{-2}° K at distances $L \approx 2.5$ cm apart in the incubator would not be sustained. Substituting even these extreme values gives as our criterion $Z_g^2 X_b \ll 6 \times 10^{-5}$ cm ^{3}. The inequality holds for typical values $Z_g = 10^{-2}$cm, $X_b = 10^{-1}$cm. Thus for less extreme values of H and/or ΔT, convection while the slide is within the incubator is negligible.

On the other hand, suppose the slide is subjected to an acceleration a(t) due to being moved by hand. To accelerate the medium and cells between the slide we require a viscous force corresponding to the pressure difference in Eq. (13), i.e. $F = 4v\eta L \delta y / Z_g = ma = \rho Z_g L \delta y a$, where v is the average velocity of the medium with respect to the slide. This gives $v = \rho Z_g^2 a / 4\eta$. Integrating both sides gives $\delta x = \rho Z_g^2 V / 4\eta \approx V / 4$ where δx is the displacement of medium relative to the slide and V is the final velocity of the slide relative to the lab. Even for quite slow velocities $V \approx 1$ cm sec^{-1} we get $\delta x \approx 1/4$ cm $= 2500 \mu m$. After handling, displacements of this order of magnitude are sometimes observed in sandwiches of large gap size, $\sim 300 \mu$m, for the loose debris of the necrotic region. After such a displacement it takes a time of order $T_c \approx 1/4$ hour before the medium returns to its normal state. Thus, handling of the sandwiches disturbs the medium gradients in a significant way and this should be recognized and minimized when designing experiments the results of which would depend critically on the details of these gradients. None of the experimental results discussed here would be so affected, and the convection acts in a way analogous to slowing down the gradient formation.

RESULTS

I. DOUBLING TIME AND OXYGEN CONSUMPTION IN MONOLAYERS

To interpret our sandwich results some background data on monolayers is needed, specifically the doubling time and the oxygen consumption. No difference was found for the doubling time, T_d, or the utilization of glucose and lactic acid by the 9L cells when they were grown conventionally in monolayer on plastic petri dishes or in monolayer on glass slides. A T_d of 13.1 hr was observed over the range of exponential growth (Fig. 8) for the 9L subculture used in all studies except the radiation studies. The cells used for the radiation studies are from a different frozen stock and the T_d for these cells is 16 hr (Fig. 17). The glucose consumption per cell, λ_G, and lactic acid production per cell, λ_{LA} over this range were computed from the cell number measurements and concentration measurements Figs. 8 and 9. The average values were $\lambda_G = 6.2 \pm 1 \times 10^{-13}$ mol/cell-hr, in agreement with Li's (1982) value for the same cell line, and $\lambda_{LA} = 1.0 \pm 0.2 \times 10^{-12}$ mol/cell-hr. Similar values can also be obtained from the data of Fig. 17. The oxygen consumption rate Q over this range was calculated assuming that all glucose not appearing as lactic acid goes completely through oxidative phosphorylation, i.e. $Q = 6(\lambda_G - \frac{1}{2}\lambda_{LA})$. We found $Q = 7.2 \pm 1 \times 10^{-13}$moles/cell-hr.

II. THE TIME AND GAP DEPENDENCE OF THE VIABLE BORDER

As in spheroids, the sandwiches developed three distinct regions: a normal-looking (and shown to be cycling) outer region, a morphologically altered (and almost non-proliferating) middle region, and a necrotic center; the first two regions constitute the viable border. We visually studied the time development of this pattern including changes in cell density and the onset and growth of the necrotic region. We also measured the size X_b of the viable border. Sandwiches of different gap sizes all showed qualitative similarities, provided we kept the gap size within the workable range for our cell line.

After setup all cells go through one to several doublings (the number depending on gap size). Then a central necrotic region appears abruptly and a sharp demarcation between live and

dead cells is observed. At this time one observes a gradient in the cell density (cells/area) over the viable border; cells are more dense at the outer edge of the sandwich and less dense near the necrotic center. Cells adjacent to the necrotic region become elongated, appear pigmented and are presumably stressed; these cells form the middle region. With time the necrotic region expands (i.e. X_b decreases; see Fig. 10) and the density of cells in the viable border increases. About 4 days after set-up the outer cells become confluent; at about this time a final viable border size is reached.

Fig. 10 shows the time dependence of X_b for the case of a 75μm gap. It also shows the time dependence of the distance from the outside of the slide to the start of the stressed (i.e. middle) region. We will call this distance X_s; in other words $X_b - X_s$ is the width of the stressed region. The initial time dependence of X_s was fit by linear regression on a semi-log plot. This fit is analyzed in the discussion section.

Cells always form a single layer on the bottom slide. The viable border width is uniform to an accuracy of about 10% between different slides of the same gap size and within one slide the border width is independent of y to an even higher precision. Visually necrotic cells remain in place and observable during the course of experiments as long as the top slide is not removed.

Although, as stated above, the qualitative features are the same regardless of the gap size, the details can be quite different. The overall effect of increasing the gap size was to spread out effects in space and slow down the onset of necrosis. For example, in 290 μm gap sandwiches the necrotic region did not appear until 50-60 hr after setup, in contrast to the 60 μm gap preparations where the necrotic center appeared at 10 hr.

Despite differences in the details, the sandwiches all approached a near-equilibrium situation when the cell density was about $N = 8.0 \pm 1.5 \times 10^4/\text{cm}^2$. With this N the final border sizes can be estimated theoretically by using Eq. 2. These theoretical values can then be compared to the observed values. The value of f_a is 0.28±0.04 mM, the concentration of O_2 in the air saturated medium at 37°C. In our calculations we take f_c to be negligibly small, although

some spheroid work (Carlsson *et al.*, 1979; Franko & Sutherland, 1979a) found values corresponding to 10-40 mm Hg. for this quantity. Even setting f_c equal to 40 mm Hg. in our calculations would have only a minor influence on our calculated final border sizes. The diffusion constant of 0_2, $D = 2 \times 10^{-5} cm^2/sec$. In choosing a value of Q, we should not naively use the consumption rate for exponentially growing cells since many of the cells are quiescent, and it has been shown for spheroids that the inner cells have a lower oxygen consumption rate (Carlsson *et al.*, 1979). Freyer *et al.* (1984) found in spheroids that the average value of Q was 1/4 that for exponentially growing cells. In our sandwich system we expect that, as is the case in spheroids, the average Q should be less than the average Q for exponentially growing monolayers. If we adopt the factor of 1/4, and use the consumption rate for exponential growth given in the earlier section describing control monolayer results, our consumption rate Q becomes $Q = 1.8 \pm 0.2 \times 10^{-13} mol/cell\ hr$. For the case of $Z_g = 60 \mu m$ this gives $X_b = 1300 \pm 100 \mu m$ compared to an observed value which is also $1300 \pm 100 \mu m$. The values for the three other gap sizes tested also show this close agreement between prediction and observation. This analysis remains valid even if, as suggested by some of our observations, there is a lag between the time the oxygen concentration reaches f_c and the onset of necrosis (in general, time lags should be easier to observe in sandwiches than in spheroids).

The observed values of the final, near-equilibrium border widths are shown in Fig. 11. The solid curve is a linear regression fit on a logarithmic scale for ease of later comparison with Eq. 2. The slope is 0.53 compared to the slope of 0.50 predicted by Eq. 2. If we take the more realistic view that Q is not constant, i.e. is not x independent in the final situation, a slope of approximately 0.50 is nonetheless predicted by the theory, as discussed in subsection I.B of the Theory section above.

III. LABELLING INDEX IN SANDWICHES

The two main qualitative results of the labelling experiments were the following: all sandwiches show a decrease in labelled cells as one moves inward on the slide; moreover, the details of this decrease depend on the sandwich gap size. One experiment is shown here to

exemplify these findings, which extend to all our labelling experiments. Sandwiches of 60 μm, 180 μm, and 290 μm gap heights were labelled 48 hr after setup. At this time the region over which live cells were found varied greatly in width for sandwiches of different gap sizes. Those of 60 μm and 180 μm gaps showed viable borders approximately 3000μm and 5200μm respectively. The 290 μm gap sandwiches had no necrotic region after 48 hr: live, attached cells were found across the whole slide. At 48 hr none of the borders had reached confluence. The absence of confluence enabled us to look at changes in the TLI due to media gradients without the complication of cells leaving cycle due to confluence.

The cells held their place well on the slide through the entire process of autoradiography. In fact, after labelling, the distance to the region where no cells remained on the slide was 3000 μm and 5000 μm for the 60 μm and 180 μm gap slides respectively, in good agreement with the observation of viable borders. Visually, it was possible to notice a definite gradient of labelled cells over the entire viable region of the sandwiches. Control monolayers showed no such gradient. Fig. 12 shows the TLI *versus* distance into the sandwich. Note that at the outer edge, $x=0$, of all sandwiches the TLI is roughly the same, corresponding to the TLI of 45% that was seen in control monolayers. All sandwiches show a steady decrease in the TLI to essentially 0% as one moves from the outside edge of the slide to the inner necrotic region, that is from $x=0$ to $x=X_b$. Although 290 μm gap sandwiches do not develop a necrotic region until 50-60 hr, the labelling index drops to 0% at 7000 μm. The smallest gap shows the steepest gradient of labelled cells and the largest gap has the least steep gradient.

The curves shown are least square fits to quadratic functions, the slope of which is constrained to be zero at the point where there are no more live cells. This choice of fitting curves is suggested by the model of the preceding section and is discussed in the next section.

For the sandwiches with a 290 μm gap an additional phenomenon was observed. For distances x greater than 3500 μm the average number of grains per labelled cell decreased. This may be due to differences in the intracellular nucleotide pools. That is, before the lid is removed, redistribution of nucleotides from the breakdown of cells in the central region could

occur; these nucleotides might be available to the salvage pathway of nearby cells, diluting the effect of the added [^{3}H]TdR.

IV. CELL CYCLE DISTRIBUTIONS IN SANDWICHES

Using flow cytometry the cell cycle distributions in sandwiches are found to be between those for exponential and confluent monolayers, and the percentage of cells with a G_1 DNA content is found to increase as the sandwich ages. Similar results have been reported for spheroids (Allison *et al* 1983).

At setup, slides with an exponentially growing cell population (Fig. 13a) are divided into two groups; the sandwiches and the controls. In time the cell cycle distribution for sandwiches then deviates from the exponential pattern (Fig. 13b). Analysis of this FACS data (as discussed in the methods section) gave the results in Table 1. We also include the data for 60μm gap sandwiches at 22.5 hr and that for confluent cultures for purposes of comparison. The decrease in S observed for the sandwiches is not a confluence effect. The 39 hour sandwiches exhibit no visible confluence. Moreover, at 39 hours the control monolayers are still in the exponential growth phase (Fig. 8) and exhibit an exponential cell cycle distribution when analyzed by flow cytometry. The fact that 24% of the cells are in S for 60μm sandwiches at 39 hr appears consistent with the labelling indices shown in Fig. 12 for the 60μm sandwiches at 48 hr.

V. RADIOSENSITIVITY OF INTERIOR VS. EXTERIOR BORDER CELLS IN SANDWICHES

When examining the radiation sensitivity of the cells in different regions of the sandwich after removal of the top slide, it was found that the cells near the necrotic center are more radioresistant than those near the nutrient source. That is, the interior border cells show an increased radioresistance compared to the exterior border cells, (Fig. 14), even though these cells are oxygenated at the time of irradiation. The onset and time dependence of this increased resistance was checked by irradiating sandwiches at different times after setup, as described in more detail below.

Sandwiches of different gap sizes were irradiated at various times after setup, but always after the necrotic center had become established. At the time of irradiation, the interior portion of the viable border was less dense than the exterior portion of the viable border. Following the irradiation the interior border cells were separated from the exterior border cells, in the manner described earlier (Methods section). When survival curves for the interior and exterior cell populations of the viable border were examined, it was found that the radiation response depended on the age of the sandwich. The radiation resistance and plating efficiency of the two populations was similar if they were irradiated shortly after the onset of the necrosis. With time, the resistance of the interior cells increased and their plating efficiency dropped. Fig. 14 shows this increased survival of the interior border cells. At still later times, the plating efficiency of the exterior border cells dropped somewhat and their resistance increased, following the trend seen for the interior population. To check these results, the survival of the whole viable border population was also examined. The survival curves for the whole border population always fell between the survival curves of the interior and exterior border populations.

An experiment was done to determine whether the increased radioresistance seen for the interior of the sandwich could be due to the selection of a resistant subpopulation. This was done as follows: after irradiation and separation into the two populations in the manner described above, the cells were plated into flasks and allowed to grow colonies for the time normally given in a radiation experiment, 11 days. The surviving colonies were then irradiated, plated, and incubated for another 11 days. Colonies from this second irradiation were counted and the survival calculated. No increase in radiation resistance was seen for the cells that were derived from interior border cells as compared to those derived from exterior border cells; both cases now had the radioresistance and plating efficiency of an exponential monolayer. Therefore, it can be concluded that the original interior border cells exhibiting increased survival were not from a resistant subpopulation.

VI. X-RAY RESPONSE OF UNFED MONOLAYERS

In order to see if the increased resistance observed for the interior of sandwiches was a condition brought about by nutrient deprivation, the radiation response of nutritionally deprived non-sandwich monolayer cells was examined.

As described earlier (Methods section), cells were grown in monolayer for up to 10 days without supplementing or changing the medium. As a result, the cells became progressively more and more starved. Every day a batch of these monolayer flasks was irradiated. In this way, a series of survival curves was obtained, from survival curves for exponentially growing cultures through those for nutrient starved plateau cultures.

There is little change in the survival curves of the unfed cells for the first 5 days. However, at the 6th day the survival curves begin to shift toward the direction of increased survival. Survival for the later days, days 7-10, appears to be increased by a factor of ~1.5 over that of days 2-5. This can be seen in Fig. 15, which shows the average survival for the early days (2-5), and the average survival for the late days (7-10). Each point shown represents the average survival at that dose for the four day period under consideration. Between three and five experiments were done for each of these 8 days, therefore the plotted points represent an average of 12-20 experimental values. Two linear-quadratic fitting curves have been drawn through these average points.

We see that, like cells in the interior of the sandwich, monolayer cells which were nutrionally deprived, days 7-10, showed an increase in cell survival when compared with their non-starved counterparts. But, unlike cells in the interior of the sandwich, these nutritionally deprived monolayer cells were not in a depleted oxygen environment prior to irradiation so hypoxia considerations seem irrelevant to understanding this phenomenon.

Along with the radiation resistance the plating efficiency of the unfed monolayer cells remains fairly constant for the first 5 days; the plating efficiency is about 58% during this period. Then, at about the same time one sees the beginnings of a rise in the radiation resistance of the cells, a drop in plating efficiency is observed (Fig. 16). The plating efficiency drops quite

dramatically after day 6.

In view of the low plating efficiencies, one might wonder whether the high survival may be due to a radiation resistant subpopulation which also plates well. In the previous section (Results V) we described experiments which indicate that the increased survival seen for cells in the interior of the sandwich is not due to selection of a resistant subpopulation. That type of experiment was not repeated on these unfed monolayers because we were reasonably satisfied that the experiments on sandwich cultures also addressed the monolayer case.

To better visualize the connection between radiation resistance and nutrient deprivation, the glucose and lactic acid concentrations of the medium were plotted as a function of time in culture for these irradiation experiments, Fig. 17. Also shown in the same figure are the number of cells per flask *versus* time in culture and the plating efficiency of the cells *versus* time in culture. Note that at the time the glucose is essentially exhausted from the medium, 105 hrs, the number of cells per flask levels off at $\sim 3 \times 10^6$ and exponential growth ceases. At this time the cells are visually confluent. Somewhat after this, at ~140 hrs, the plating efficiency drops, and we know from Fig. 16 that the increased radioresistance develops at about this time. Flow cytometry studies show that almost all of the cells are in a G_1 state during the later days, days 7-10.

In these experiments, the plateau phase of the cultures is brought on by the state of the medium (e.g. by a shortage of glucose, see Fig. 17), rather than by contact inhibition. By changing the medium the cells can be brought back into cycle; indeed, during the early stages of the plateau phase, even shaking the cultures for a number of hours brought them back into cycle. Moreover, on day 8 many of the cells appear rounded up and by day 9 massive cell death occurs. The cells surviving at this and later times are consequently far from confluence.

To further demonstrate that the increased survival was not a result of cell confluence we put medium depleted of glucose and lactic acid on low density exponentially growing cultures. The plating efficiency of these cultures dropped and the radiation resistance rose, as is consistent with the data for the unfed monolayer cultures.

The error in surviving fraction for these x-ray experiments was calculated by taking the standard deviation of replicate experiments done at different times, and is represented by the error bars in Figs. 15 & 16. The error was also calculated by taking the standard deviation of 9 replicate samples done in rapid succession on the same day. In this case the standard deviation was found to be 13%.

DISCUSSION

I. CELL CYCLE KINETICS AND DIFFUSION IN SANDWICHES

In order to better understand the cell cycle distribution and the development of a necrotic center in poorly vascularized tumors, we developed a two-dimensional, diffusion-controlled system for cell growth. The system complements the spheroid system, a three-dimensional *in vitro* tumor model. Spheroids have been widely used during the last ten years as models for the cellular kinetics (Durand 1976), the radiation response (Sutherland & Durand 1976; Durand 1980), and the growth dynamics (Franko & Sutherland 1979a; Yuhas 1978) of tumors. Spheroids are thought to mimic tumors with respect to both the nutrient diffusion gradients and the three dimensional cellular interactions; of course, spheroids have no vascularization. Phenomena that are observed in tumors and spheroids alike, but not in conventional monolayer cultures, are thought attributable to either diffusion gradients, three-dimensional contact or some combination of these. If these phenomena are also observed in sandwich cultures they should be viewed as a result of gradients, since the sandwich system does not have the three-dimensional cellular interactions present in spheroids.

The sandwich system is in this respect less like a tumor than is a spheroid, but it has the advantage that it gives optimal information on diffusion effects in growing cell populations. The amplification of the viable border by a factor of ten, compared to viable rims in spheroids of the same cell line, points to the increase in cell kinetic information available from labelling studies on sandwiches. That is, since the gradients of diffusing substances are less steep, there are many more cells within a given concentration range and one can separate out sub-populations more easily.

One also has control over the border width by simply varying the gap height. Thus one can check the causal relationship between diffusion and necrosis in a way not available in the spheroid system. We varied the sandwich gap height and observed different final border widths (Fig. 11) for the same cell line under the same initial conditions. That necrosis is the

result of diffusion limitations seems clear from the 0.53 slope observed. Not only the basic model, in which the key substance is oxygen, but also any other simple diffusion limited model predicts a 0.50 slope for that curve since Eq. (2) implies $\ln X_b = \frac{1}{2}\ln Z_g + A$, where A is independent of Z_g.

If the key substance is oxygen we can obtain a value of Q using Eq. 2 and the values $f_a = 0.28 \pm 0.04$mM, $f_c = 0$, $D = 2\times10^{-5}$cm^2/sec, $N = 8.0 \pm 1.5 \times 10^4$/cm^2 already discussed. Using the best fit line in Fig. 11 to average, we get $Q = 2f_a DZ_g / NX_b^2 = 1.65 \pm 0.3 \times^{-13}$mol/cell-hr. Since this is indeed about (1/4) the value of Q found for exponential growth, just as in spheroids (Freyer *et al.* 1984) the oxygen assumption is consistent. This value of Q should be regarded as an average for the sandwich cells; x dependent variations presumably occur, but are masked by the averaging process (compare I.B in the Theory section).

Several investigators (Mueller-Kleiser *et al.* 1983; Li 1982) have suggested that glucose, as well as oxygen may be a critical factor in the onset of necrosis under certain conditions. A calculation similar to that just given for the case of oxygen determines the glucose consumption λ_G needed to account for the observed border widths if glucose alone were the limiting factor. In contrast to the spheroid case we can use the glucose diffusion constant for medium, without considering cell packing density. We find $\lambda_G \approx 10^{-12}$mol/cell hr, i.e. about twice the value found in exponential monolayer growth for our cell line. Since glucose utilization is often higher at lower oxygen concentrations this may be a reasonable value. We can therefore not eliminate glucose deprivation as a contributory factor in the formation of necrosis, and we are currently doing further experiments to investigate its role. These experiments utilize the substitution of a plastic, oxygen permeable top slide for the glass one which is impermeable to oxygen. In this way oxygen gradients are eliminated and one has a method of separating glucose effects from oxygen effects. This method is not available in spheroids or in the tumors themselves.

The increase observed in non-cycling cells as the sandwich ages parallels the findings of non-cycling cells in large spheroids (Allison *et al.* 1983; Carlsson 1979; Durand 1976) and in

poorly vascularized tumors (Tannock 1968). Moreover, as in spheroids, the cells not only go out of cycle in time but also in distance. There is the typical decrease of cells in S as we move away from the nutrient source, reaching 0% near the necrotic region. This is shown directly by [^{3}H]TdR labelling experiments (Fig. 12). In examining Fig. 12 it is worth noting that the dependence of labelling index on the distance x into the slide can be analyzed much more closely in sandwiches than is possible in spheroids because the viable borders in sandwiches are ten times larger than the viable rims in spheroids and one need not section the sample to estimate the labelling index. Due to this extra sensitivity it makes sense to see how well our data fits the hypothesis that cells stop cycling due to low oxygen. There is indeed evidence that cells become quiescent when exposed to low oxygen (hypoxia blocks in G_1; see Koch *et al.* 1973 and also Loffler *et al.* 1978). Olivotto & Paoletti (1981) found that certain quiescent tumor cells could not be brought back into cycle unless oxygen was available. With this in mind let us return to our basic oxygen model and assume that at a given x the labelling index is simply proportional to $f(x)-f_c$, the amount by which the oxygen concentration exceeds the critical value for necrosis. Then the labelling index should depend quadratically on x; the curvature (i.e. the coefficient C of the term $\frac{1}{2}Cx^2$) should be inversely proportional to the gap width (compare Eq. 1). In Fig. 12 we have given least square quadratic fits under the constraint that the slope go to zero at an appropriate point near the necrotic center. The corresponding values of C, namely 4.7 for $Z_g=60\mu$m, 3.0 for $Z_g=180\mu$m and 0.79 for $Z_g=290\mu$m indeed decrease as the gap height increases. The lack of a direct proportionality to $1/Z_g$ may be due to the fact that labelling is not precisely proportional to the oxygen excess or may be an artifact reflecting the marked sensitivity of our fit to the exact choice of constraints. Because the borders are so wide it should be comparatively easy to supplement the data in Fig. 12 and investigate this question more closely.

Visually, the middle region of the sandwiches (between X_s and X_b) contains cells showing an altered morphology. This phenomenon of "visible stress" and that of cell quiescence are presumably closely related, though by no means identical. Thus we should also try checking

the hypothesis that cells become visibly stressed due to low oxygen. More specifically, suppose that cells show this altered morphology wherever the oxygen concentration falls below a certain value f_s, possibly after a time lag t_l, and that the consumption by cells in the middle region is negligible compared to consumption by cells in the outside region. Then we can use Eq. 2 to evaluate the behavior of X_s by replacing f_c and X_b with f_s and X_s respectively. This gives $\ln X_s(t) = -\frac{1}{2}\ln(QN) + K$ where K is time-independent and QN is evaluated at $t - t_l$. For $N = N_0 e^{\alpha t}$ with $\alpha = \ln 2/13\text{hr}$ and Q constant we have $\ln X_s = -\beta(t - t_l) + constant$ with $\beta = \ln 2/26\text{hr}$. Plotting $\ln X_s$ *versus* time in Fig. 10 we can find the empirical value of the slope β. From the fitting curve, which uses only the first three points to avoid any confluence effects, we obtain $\beta = \ln 2/32\text{hr}$. The agreement between calculated and empirical slopes is reasonable and the discrepancy could be due to the fact that Q decreases in time rather than being constant. Thus the presence of visibly stressed cells, like that of quiescent ones, might be explainable by an oxygen deprivation hypothesis.

Evidence for the increase in quiescent cells as the sandwich ages is given by the FACS data. This data, which gives results integrated over all the cells, from the outer cells to the ones nearest the necrotic center, appears consistent with the labelling data. The FACS data also shows that the decrease of cells in S is accompanied, as expected from spheroid work (Allison *et al.* 1983; Sutherland *et al.* 1971), by an increased fraction of cells in G_0/G_1.

In summary, our picture of the response of a sandwich to diffusion gradients is the following. When the top slide is put in place, gradients of oxygen, nutrients and metabolites form. These gradients offer different local environments for cells in different regions of the sandwich; the consequence is a spatial variation in the cell cycle distribution. As the cells multiply the gradients become larger. Cells in the center die, presumably from lack of oxygen. Cells adjacent to this central necrotic region appear visibly altered, go out of cycle, and ultimately also die. The size of the necrotic region expands and the density of cells in the viable border increases. We see that despite the change in geometry there are many salient features which are similar in sandwiches and spheroids but which don't appear in normal monolayer cultures. Such

features can be considered as consequences, direct or indirect, of diffusion gradients.

II. RADIATION RESPONSE

The special features of the sandwich system, such as the access to cells in all regions, make possible alternative approaches to investigating the radiation response of cells which are hypoxic due to diffusion limitations and to investigating the cell contact effect. After removal of the top slide, the different cell populations can be separated under the microscope. This circumvents the more indirect approaches of sequential trypsinization or fluorescence-activated cell sorting of populations. The top slide can be removed after an experiment to simply allow the investigator access to cells for separation purposes, or it can be removed (and replaced if desired) during the course of an experiment as a means of turning off the diffusion gradients, as we did in our x-ray experiments. In this second case the time of removal becomes another controllable parameter not available in tumors or spheroids. In our experiments we abolished the gradients, including that of oxygen, just prior to irradiation.

Our sandwich x-ray studies show that cells in the interior half of the viable border are more radioresistant than those found in the exterior half of the viable border, even when irradiated in the presence of oxygen. The resistance appears after the necrotic center has set in, and labelling studies show that most of the interior border cells are out of cycle at this time. These results suggest to us two main conclusions: that the radioresistance is due to the out-of-cycle cells having extra time to repair their damage; and that the increased radioresistance of the 9L spheroids, which is often attributed to the cell contact effect, may be due, at least partially, to the effects of a more radioresistant noncycling subpopulation. We next discuss the first of these two implications.

This idea that cells utilize extra cell cycle time to repair their damage is an explanation often given for the increased survival after delayed plating in potentially lethal damage (PLD) repair experiments. In these experiments the cells are prevented from normally cycling for a number of hours after the irradiation. Such PLD studies have recently been done on 9L cells (Rodriguez and Alpen, private communication). There are similarities between the results of

these PLD experiments, our results for sandwiches and our results for starved monolayers. The similarities suggest that a single interpretation may well apply to these various sets of data, despite the fact that our cells, unlike those in the PLD experiments, were in depleted medium prior to irradiation and were plated immediately afterwards.

In the Rodriguez-Alpen PLD experiments 9L cells from spheroids and from monolayers are held in depleted medium, for 5-24 hours after irradiation. Cells which were not held in depleted medium, but rather immediately plated, were examined as controls. The survival curves for the delayed platings from spheroids and monolayers are similar to each other despite the fact that spheroids show extra radioresistance in the immediate plating experiments. Moreover, these survival curves are similar in shape and values to the survival curves we obtained, using the same cell line, for both the sandwich interiors and the day 7-10 starved monolayers (Figs. 14 & 15). Thus, we see that the survival in different experiments is similar under conditions that lead to increased cellular radioresistance. So perhaps the high survival seen for the sandwich interiors and the day 7-10 monolayers is due, like that seen in delayed plating experiments, to having extra time to repair. This extra time to repair is conjectured to arise in cells which were blocked in G_1. Such cells are presumed to undergo a lengthening of G_1 by several hours upon resumption of cycling brought on by plating in fresh medium. There is a substantial amount of literature attesting to the fact that for many cell lines noncycling cells from "starved" plateau cultures accumulate primarily in G_1 and that once cycling resumes G_1 is indeed several hours greater than in normally cycling cells (Nelson, Todd & Metting, 1984; Brooks, 1976). Note here that our cells should be compared to "starved" plateau monolayers rather than ones whose growth is contact inhibited, since neither the interior of our sandwiches nor our monolayer cultures are fully confluent at the time of maximum radioresistance.

The idea that the radioresistance we see stems from the cells being out of cycle and therefore having more time to repair is supported by the fact that the literature shows plateau cultures to be more radioresistant. This is true even for cell lines in which G_1 is not the most

radioresistant part of the cell cycle, so the increase in resistance is probably not attributable to just synchronization in G_1, but rather the elongation of the cell cycle before some critical event. In our own experiments on unfed monolayers, exponential growth ceases shortly before the radiation resistance of the cells begins to rise (Figs. 16 & 17), lending credence to the idea that being out of cycle correlates with time to repair.

Time to repair seems a good working explanation for the phenomena of extra radioresistance in our experiments. If the explanation is valid it presumably applies more generally to the interior cells of spheroids and tumors of other cell lines. However, it is possible that the increased survival we see may not be a generalized finding, but rather be specific for the 9L cell line.

Indeed, by pushing all the adjustable parameters to the limit, we might just explain the increased resistance as due to cell cycle effects, despite the fact that the age response of 9L cells is comparatively flat. Using the 9L age response data from Kimler & Henderson, 1982, and the cell cycle parameters from Sweigert, 1984, we can make the following estimates for an exponentially growing 9L cell population: about 10% of the cells are in a very radiosensitive M state (essentially no survival, even at a dose of 400 rad); about 70% are in a state somewhat less resistant than the maximally resistant state (about 1.4 as many deaths as for cells at the maximum survival part of the cell cycle); and the remaining 20% of the cells are in the maximally resistant state, which occurs during G_1. Now suppose that all the starved cells are blocked not simply in G_1, but in the most resistant part of G_1, which is the middle part of G_1. Then the survival rate for starved cells is $1/[0.2\times1 + 0.7\times(1/1.4) + 0.1\times0]\approx1.4$ times the survival rate for an exponentially cycling cell population. While our data indicate a discrepancy factor of 1.5 rather than 1.4, empirical inaccuracies might well account for the balance. But we must remember that to get a factor of 1.4 we had to assume all the cells were blocked in the most resistant half of the G_1 state and we have no evidence that this is the case. If the cells were actually blocked in early or late G_1 survival should be no greater than in an exponentially growing cell population, as a corresponding calculation shows.

Another indication that the effects may be specific to the 9L cell line are the results of Durand (1983). He labelled whole V79 spheroids with Hoechst 33342, a nontoxic fluorescent stain, and then using flow cytometry separated interior cells from exterior cells according to their uptake. The survival curves for these two populations show the interior cells more sensitive to irradiation when considerations of hypoxia have been eliminated.

This brings us to our second conclusion, that the increased radioresistance seen for 9L spheroids and attributed to the "cell contact effect" may actually be due to a more radioresistant noncycling subpopulation.

As is well known, in many cases tumor and spheroid cells show an increased radioresistance when the tumor or spheroid is irradiated intact rather than in a disassociated state (Steel, 1973; Wallen *et al,* 1980; Rockwell & Kallman, 1973; Durand & Sutherland, 1973; Rasey, 1983). It has been hypothesized that this increased resistance stems from three-dimensional cell to cell contact, perhaps being due to cooperative effects between the cells (Durand & Sutherland 1972; Durand & Sutherland 1973; Dertinger, Hinz & Jacobs 1982).

Our sandwich results seem to indicate that in 9L spheroids an increased radioresistance due to three-dimensional cell contact, if it occurs at all, is smaller than previously thought. That is, in light of our data it appears that the increased radioresistance seen for 9L cells irradiated as intact spheroids (Rodriguez & Alpen, 1981) is at least partially due to a more radioresistant noncycling subpopulation. In our x-rayed sandwich cultures we saw an increased resistance for the interior border cells. These cells did not have three-dimensional cell contact or even strong two-dimensional contact. If one assumes that such a radioresistant subpopulation also occurs in the 9L spheroid by virtue of a like cause, diffusion gradients, this line of reasoning sheds doubt on the importance of three-dimensional contact in the radioresistance of 9L spheroids.

One of course needs to check other cell lines to see if our finding has a more generalized significance. Work on spheroids of the B14 line (Dertinger & Hulser; 1981) has shown that the "contact effect" is not due to a noncycling subpopulation in that cell line, since even cells from the outer proliferating layer of the spheroid show the "contact effect". In any case, it seems likely that use of the sandwich system will help clarify the role of the "contact effect".

GLOSSARY

We list some key words and symbols, together with a reference in brackets to the place or places where more detailed information on each can be found.

Border; Viable border. After a sandwich has developed a necrotic region, the regions in which the cells are still alive is referred to as the viable border; analogous to the viable rim of a spheroid. [Materials and Methods I; Fig. 1].

D. Diffusion constant, usually that for oxygen in water. [Theory I.A].

Exterior; Exterior border cells. The outside part of the viable border; usually about ½ of the viable border in width. [Materials and Methods VI.B; Fig. 3].

f. The concentration of some key substance, usually oxygen, in the sandwich medium. [Theory I; Fig. 4].

f_a. The ambient oxygen concentration. More specifically, the oxygen concentration of the medium just outside the sandwich. [Theory I.A; Fig. 4].

f_c. The critical oxygen concentration, theoretically low enough that cells become necrotic. [Theory I.A; Fig. 4].

f_s. An oxygen concentration, theoretically low enough that cells become visibly stressed. [Discussion I].

Gap. The region between the two glass slides of a sandwich. [Materials and Methods II].

Interior; Interior border cells. The part of the viable border next to the necrotic region; usually about ½ of the viable border in width. [Materials and Methods VI.B].

λ_G. The glucose consumption rate. [Results I; Fig. 9].

λ_{L4}. Lactic acid consumption rate. [Results I; Fig. 9].

n. Number of cells per unit volume. [Theory I.A].

N. Number of cells per unit area. [Theory I.A].

Q. Consumption rate of some substance, usually oxygen. [Theory I.A].

Setup; setup time. The time at which the top slide of a sandwich is added; the origin t=0 in the graphs is usually taken as the setup time. [Materials and Methods II; Fig. 3].

TLI. Thymidine labelling index. [Materials and Methods IV].

T_b. The time for oxygen to diffuse a distance equal to the distance from the outside of a sandwich to the necrotic region. [Theory I.A].

T_c. The time for a cell to consume all the oxygen in its own "allotted space", assuming no replenishment. [Theory I.A].

T_d. The cell doubling time. [Theory I.A].

T_g. The time for oxygen to diffuse a distance equal to the gap height of a sandwich. [Theory I.A].

Viable border. See border.

x. Distance into a sandwich, going from the region where cells have free access to nutrients toward the necrotic center. [Materials and Methods II; Fig. 1].

X_b. Width of the viable border. [Materials and Methods III; Fig. 4].

X_s. Width of that part of the viable border that does not appear visually stressed. [Results II; Fig. 10].

y. The distance along a sandwich. Normally all quantities are y independent, except for end effects. [Materials and Methods II; Fig. 1].

z. Vertical distance; perpendicular to the plane of the slide. [Materials and Methods II; Fig.1].

Z_g. The height of the gap between the top slide and the bottom slide in a sandwich. [Fig. 1].

BIBLIOGRAPHY

Allison, D.C., Yuhas, J.M., Ridolpho, P.F., Anderson, S.L. & Johnson, T.S. (1983) Cytophotometric measurement of the cellular DNA content of [^{3}H] thymidine-labelled spheroids. *Cell Tissue Kinet.* **16,** 237.

Brooks, R.F. (1976) Regulation of the fibroblast cell cycle by serum. *Nature* **260,** 248.

Burton, A.C. (1966) Rate of growth of solid tumors as a problem of diffusion. *Growth,* **30,** 157.

Carlsson, J., Stalnacke, C.G., Acker, H., Haji-Karim, M., Nilsson S. & Larsson, B. (1979) The influence of oxygen on viability and proliferation in cellular studies. *Int. J. Radiation Oncology Biol. Phys.* **5,** 2011.

Conger, A. & Ziskin, M. (1983) Growth of mammalian multicell tumor spheroids. *Cancer Res.* **43,** 556.

Dawson, K. (1973). *Europ. J. Cancer* **9,** 59.

Dean, P.N. & Jett, J.J. (1974) Mathematical analysis of DNA distributions derived from flow microfluorometry. *J. Cell Biol.* **60,** 523.

Deen, D.F., Hoshino, T., Williams, M., Muraoka, I., Knebel, K. and Barker, M. (1980) Development of a 9L rat brain tumor cell multicellular spheroid system and its response to 1.3-bis(2-chloroethyl)-l-nitrosourea and radiation. *J. Natl. Cancer Inst.* **64,** 1373.

Dertinger, H., Guichard, M & Malaise, E.P. (1983) Is there a relationship between hypoxia, contact resistance and intercellular communication? Radiat. Environ. Biophys. **22,** 209.

Dertinger, H., Hinz, G. & Jacobs, K.H. (1982) Intercellular communication, 3-dimensional cell contact and radiosensitivity. *Biophys. Struct. Mech.* **9,** 89.

Dertinger, H. & Hulser, D (1981) Increased radioresistance of cells in cultured multicell spheroids. I. Dependence on cellular interaction. *Radiat. Environ. Biophys.* **19,** 101.

Dethlefsen, L.A. (1980) In quest of the quaint quiescent cells. In: *Radiat. Biology in Cancer Research*, eds. R Meyn and H.R. Withers, Raven Press, NY.

Durand, R.E. (1975) Isolation of cell subpopulations from *in vitro* tumor models according to sedimentation velocity. *Cancer Res.* **41,** 1295.

Durand, R.E. (1976) Cell kinetics in an *in vitro* tumor model *Cell Tissue Kinet.* **9,** 403.

Durand, R.E. (1980) Variable radiobiological responses of spheroids. *Radiat. Res.* **81,** 85.

Durand, R.E. (1982) Use of Hoechst 33342 for cell selection from multicell systems. tumor model *J. Histochem. Cytochem.* **30,** 111.

Durand, R.E. (1983) Oxygen enhancement ratio in V79 spheroids. *Radiation Res.* **96,** 322.

Durand, R.E. & Sutherland, R.M. (1972) Effects of intercellular contact on repair of radiation damage. *Exp. Cell Res.* **71,** 75.

Durand, R.E. & Sutherland, R.M. (1973) Growth and radiation survival characteristics of V79-171b Chinese Hamster cells: A possible influence of intercellular contact. *Radiation Res.* **56,** 513.

Fabrikant, J.I., Wisseman, C.L. & Vitak, M.J. (1969) The kinetics of cellular proliferation in normal and malignant tissues. An *in vitro* method for incorporation of tritiated thymidine in human tissues. *Radiology* **92,** 1309.

Franko, A.J. & Sutherland, R.M. (1978) Rate of death of hypoxic cells in multicell spheroids. *Radiat. Res.* **76,** 561.

Franko, A.J. & Sutherland, R.M. (1979a) Oxygen diffusion distance and development of necrosis in multicell spheroids. *Radiat. Res.* **79,** 439.

Franko, A.J. & Sutherland, R.M. (1979b) Radiation survival of cells from spheroids grown in different oxygen concentrations *Radiat. Res.* **79,** 454.

Freyer, J.P. & Sutherland, R.M. (1980) Selective dissociation and characterization of cells from different regions of multicell tumor spheroids. *Cancer Res.* **40,** 3956.

Freyer, J.P., Tustanoff, E., Franko, A.J. & Sutherland, R.M. (1984) In situ Oxygen consumption rates of cells in V-79 multicellular spheroids during growth. *J. Cell. Physiol.* **119,** 53.

Frindel, E., Malaise, E.P., Alpen, E.& Tubiana, M. (1967) Kinetics of cell proliferation of an experimental tumor. *Cancer Res.* **27,** 1122.

Giesbrecht, J.L., Wilson, W.R. & Hill, R.P. (1981) Radiobiological studies of cells in multicellular spheroids using a sequential trypsinization technique. *Radiat. Res.* **86,** 368.

Greenspan, H.P. (1972) Models for the growth of a solid tumor by diffusion. *Stud. Appl. Math.* **51,** 317.

Hill, R.P. (1980) An appraisal of *in* vivo assays of excised tumours. *Br. J. Cancer* **41,** 230.

Hill, R.P., Ng, R., Warren, B.F. & Bush, R.S. (1979) The effect of intercellular contact on the radiation sensitivity of KHT sarcoma cells. *Radiat. Res.* **77,** 182.

Hlatky, L. & Alpen, E.L. (1985) Two dimensional diffusion limited system for cell growth. *Cell Tissue Kinet.* **18,** 000.

Kim, J.H., Kim, S.H., Perez, A.G. & Fried, J. (1973) Radiosensitivity of confluent density-inhibited cells. *Radiology* **106,** 447.

Kimler, B.F. & Henderson, S.D. (1982) Cyclic responses of cultured 9L cells to radiation. *Rad. Res.* **91,** 155.

Koch, C.J., Kruuv, J., Frey, H.E. & Snyder, R.A. (1973) Plateau phase in growth induced by hypoxia. *Int. J. Radiat. Biol.* **1,** 67.

Leith, J.T., Schilling, W.A. & Wheeler, K.T. (1975) Response of a rat brain tumor. *Cancer* **50,** 1545.

Li, C.K.N. (1982) The glucose distribution in 9L rat brain multicell tumor spheroids and its effect on cell necrosis. *Cancer* **50,** 2066.

Loffler, M., Postius, S. & Schneider, F. (1978) Anaeobiosis and oxygen recovery: changes in cell cycle distribution of Ehrlich ascites tumour cells grown *in vitro*. *Virchows Arch. B Cell Path.* **26,** 359.

McNally, N.J. & De Ronde, J. (1980) Radiobiological studies of tumours *in situ* compared with cell survival. *Br. J. Cancer.* **159,** Suppl. IV, 259.

Mueller-Kleiser, J.P., Freyer, J.P. & Sutherland, R.M. (1983) Evidence for a major role of glucose in controlling development of necrosis in EMT6/Ro multicell tumour spheroids. *Advances Exp. Med. Biol.; Oxygen Transport to Tissue – IV* **159,** 487.

Mueller-Kleiser, J.P. & Sutherland, R.M. (1982) Influence of convection in the growth medium on oxygen tensions in multicellular tumour spheroids. *Cancer Res.* **159,** 237.

Nelson, J.M., Todd,P. & Metting, N.F. (1984) Kinetic differences between fed and starved Chineses hamster ovary cells. *Cell Tissue Kinet.* **17,** 411.

Olive. P.L. & Durand R.E. (1985) Effect of intercellular contact on DNA conformation, radiation induced DNA damage, and mutation in Chinese Hamster V79 cells. *Radiat. Res.* **101,** 94.

Olivotto, M. & Paoletti, F. (1981) The role of respiration in tumor cell transition from the noncycling to the cycling state. *Journal of Cellular Physiology* **107,** 243.

Rajewsky, M.F. (1965) *In vitro* studies of cell proliferation in tumours. *Europ. J. Cancer* **1,** 281.

Rasey, J.S. (1983) Cell-cell contact and repair of radiation damage (review). *Proc. ICRR 7* **Review Volume,** 303.

Rockwell, S. & Kallman, R.F. (1973) Cellular radiosensitivity and tumour radiation response in the EMT6 tumour cell system. *Radiat. Res.* **53**, 281.

Rodriguez, A. & Alpen, E.L. (1981) Cell survival in spheroids irradiated with heavy-ion beams. *Radiat. Res.* **85**, 24.

Rubin, H. & Rein, A. (1967) Proximity effects in the growth of animal cells. In: *Growth Regulating Substances for Animal Cells in Culture (Wistar Institute Symposium Monograph 7)* V. Defendi and M. Stoker eds., Wistar Ins. Press, Philadelphia.

Steel, G.G. (1977). *Growth Kinetics of Tumors,* Oxford University Press.

Sutherland, R.M., McCredie, J.A. & Inch, W.R. (1971) Growth of multicell spheroids in tissue culture as a model of nodular carcinomas. *J. Natl. Cancer Inst.* **46**, 113.

Sutherland, R.M. & Durand, R.E. (1973) Hypoxic cells in an *in vitro* tumour model *Int J. Radiat. Biol.* **23**, 235.

Sutherland, R.M. & Durand, R.E. (1976) Radiation response of multicell spheroids – an *in vitro* tumour model. *Curr. Top. Radiat. Res.* **11**, 87.

Sutherland, R.M. & Franko, A.J. (1980) On the nature of the radiobiologically hypoxic fraction in tumors. *Int. J. Radiat. Oncol. Biol. Phys.* **6**, 117.

Sweigert, S. (1984) Cell proliferation kinetics and radiation response in 9L tumor spheroids. *Ph.D. Dissertation, Univ. Cal. Berkeley.*

Tannock, I.F. (1968) The Relation between Cell Proliferation & the Vascular System in a Transplanted Mouse Mammary Tumor. *Brit. J. Cancer* **22**, 258.

Thomlinson, R.H. & Gray, L.H. (1955) The Histologic Structure of some Human Lung Cancers and the Possible Implications for Radiotherapy. *Brit. J. Cancer* **9**, 539

Tobias, C.A., Blakely, E.A., Ngo, F.Q.H. & Yang, T.C.H. (1980), The repair-misrepair model of cell survival. *Radiation Biology and Cancer Research* A. Meyn and R. Withers, eds. New

York: Raven Press 195.

Vindelor, L.L., Christensen, I.J. & Nissen, N.I. (1983) A detergent-trypsin method for the preparation of Nuclei for flow cytometric DNA analysis. *Cytometry* **Vol. 3,** 323.

Wallen, C.A., Michaelson, S.M. & Wheeler, K.T. (1980) Evidence for an unconventional radiosensitivity of rat 9L subcutaneous tumours. *Radiat. Res.* **84,** 529.

Yuhas, J.M., Li, A.P., Martinez, A. & Ladman, A. (1977) Cell loss and influx of labeled host cells in three transplantable mouse tumors using [^{125}I]UdR release. *Cancer Res.* **37,** 3639.

Yuhas, J.M.& Li, A.P. (1978) Growth fraction as the major determinant of multicellular tumor spheroid growth rates. *Cancer Res.* **38,** 1528.

LEGENDS

Fig. 1. Schematic of sandwich system. (a) Top view, showing two sandwiches in a Petri dish, with holders (cross-hatched) and spacers (solid black) at the left and right ends. Note the axes. The shaded region in the lower sandwich denotes the necrotic center; the dashed line divides the viable border into the two visibly different regions. (b) Edge view, showing the medium-filled gap between slides and cells attached to the bottom slide.

Fig. 2. X- ray survival curves for 9L monolayers irradiated on plastic ■ and on glass □ . The effective dose on glass is 1.5× the dose on plastic.

Fig. 3. The procedure used to oxygenate sandwiches and to separate their interior from their exterior border cells during the radiation experiments.

Fig. 4. Theoretical oxygen concentration as a function of distance x into the sandwich. f_a is the concentration at the edges of the slide (e.g. at $x=0$). Note that the oxygen profile is flat in the necrotic region, where there are no consuming cells.

Fig. 5. Geometry used in calculating the local oxygen depletion near the edge of a sandwich. Oxygen flux is indicated by arrows.

Fig. 6. Geometry used to estimate vertical diffusion rates in sandwiches. Z_1 is the height of the cell layer, Z_1+Z_2 is the total gap height Z_g. The oxygen concentration is taken to be f_1 for $0 \le z < Z_1$ and taken to be f_2 in the upper part of the gap $Z_1 \le z \le Z_g$.

Fig. 7. Geometry used in the calculation estimating convection in sandwiches. We assume a slight tilt and a slight temperature gradient while the slide is in the incubator. Arrows indicate possible direction of the convective currents.

Fig. 8. The growth curve of 9L cells. The points in the exponential region were fit by linear regression. This plot reflects three experiments. The standard deviation was within the plotted points.

Fig. 9. Glucose (□) and lactic acid (×) concentrations for the exponential and confluent growth of 9L cells in monolayer. When no error bar is shown the standard deviation lies within the plotted points.

Fig. 10. Border widths X_b (○) and X_s (●) as functions of time. The first three points for X_s were fit by linear regression.

Fig. 11. Final border width as a function of gap size. Each point represents 15 replicate samples.

Fig. 12. Labelling index *versus* distance into the sandwich for 60μm (○), 180μm (+) and 290μm (□) gap sandwiches, all at 48 hr. Arrows indicate the start of the necrotic region for the 60μm and 180μm cases. At 48 hr the 290μm sandwiches show no necrotic center. The standard deviations were within the plotted points.

Fig. 13. Representative DNA histograms for (a) exponentially growing cells and (b) 60μm gap sandwiches at 39 hr. Each histogram represents a total of 10^5 cells. The coefficients of variation were less than 4%.

Fig. 14. Survival curves for interior and exterior border cells in an oxygenated sandwich. Each point reflects experiments done on five different days. The doses shown are those actually measured by the Victoreen and not corrected for the extra dose from the glass backscatter.

Fig. 15. Survival curves for unfed monolayers. The lower curve is an average for monolayers during days 2-5; the upper curve shows the corresponding data for days 7-10. The curves are computer generated linear-quadratic fits. In comparing to Fig. 14 the factor of 1.5 between plastic and glass should be taken into account.

Fig. 16. The upper graph shows % survival at 400 rads, normalized by the appropriate plating efficiency, *vs.* time for unfed monolayers. The curves at doses higher than 400 rads have the same general shape. The lower graph shows the plating efficiency *vs.* time for unfed

monolayers.

Fig. 17. Data for unfed monolayers during the ten day period. If no error bar is shown the error is within the plotted point. Note that the cells reach plateau phase and the plating efficiency begins to drop at about the same time the medium is depleted of glucose.

Table 1. Cell-cycle distributions; based on DNA content analysed by flow cytometry.

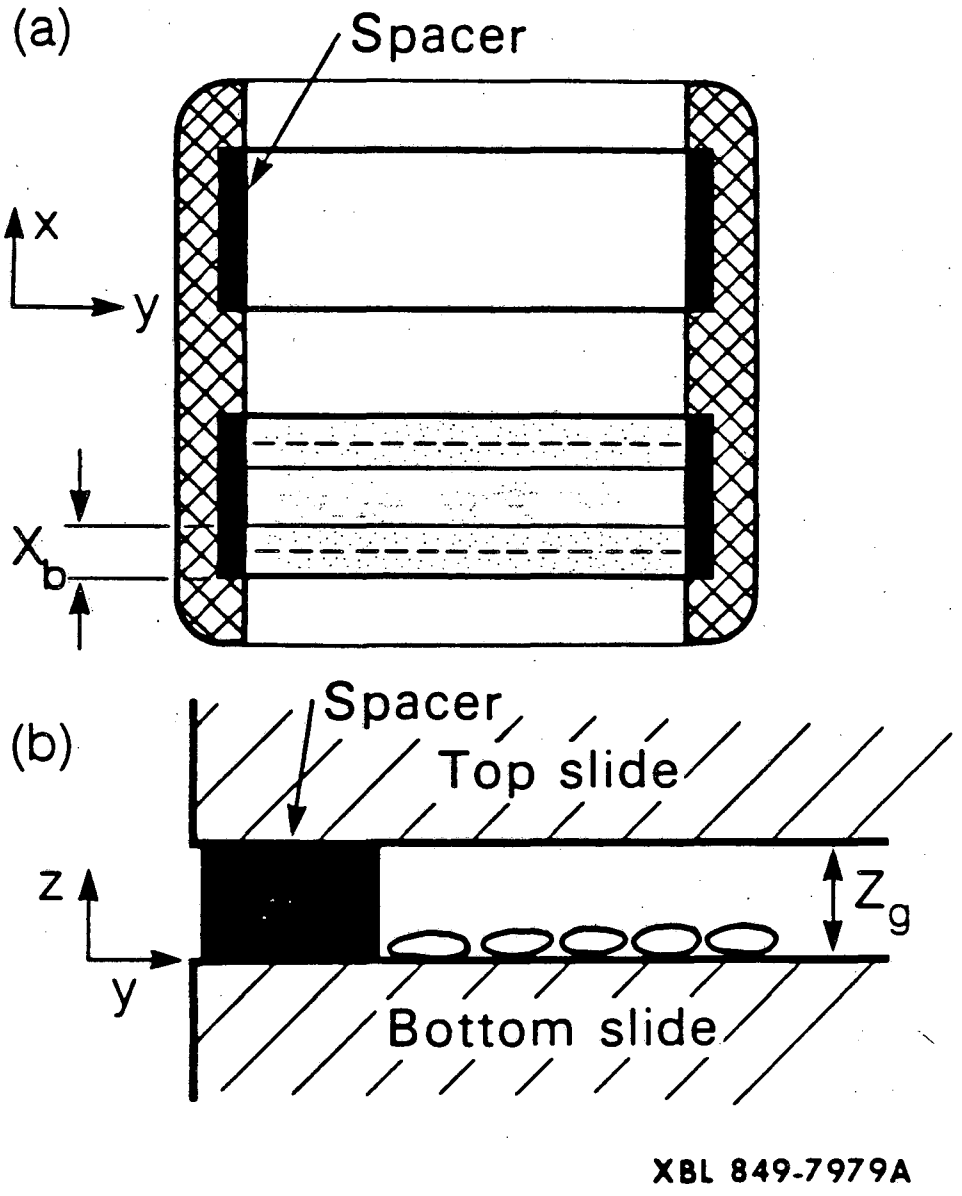
(a)
Spacer
x
y
X_b
(b)
Spacer
Top slide
z
y
Z_g
Bottom slide
XBL 849-7979A

Fig. 1

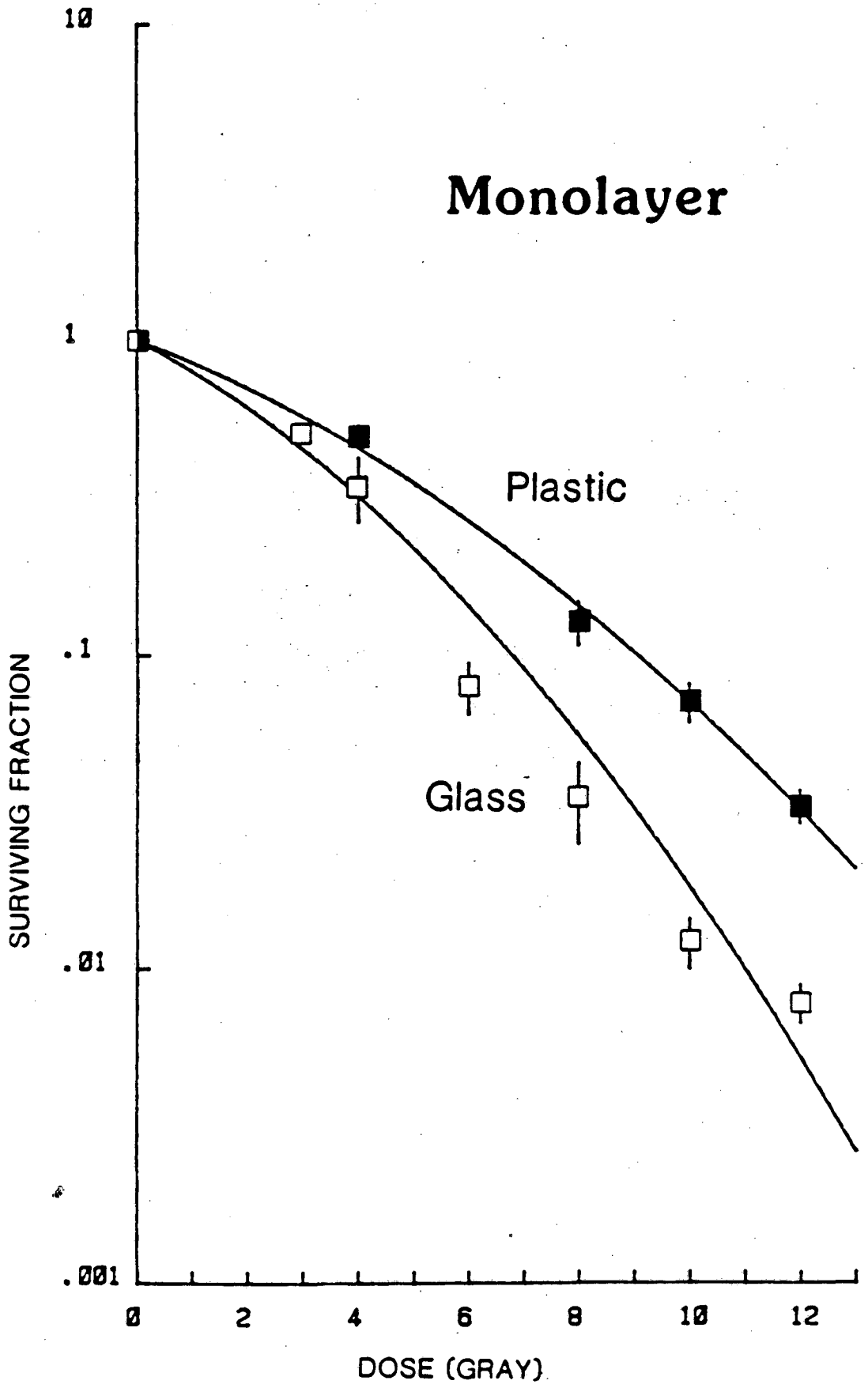
Monolayer
Plastic
Glass
SURVIVING FRACTION
10
1
.1
.01
.001
0
2
4
6
8
10
12
DOSE (GRAY)

Fig. 2

INTERIOR VERSUS EXTERIOR BORDER X-RAY PROCEDURE

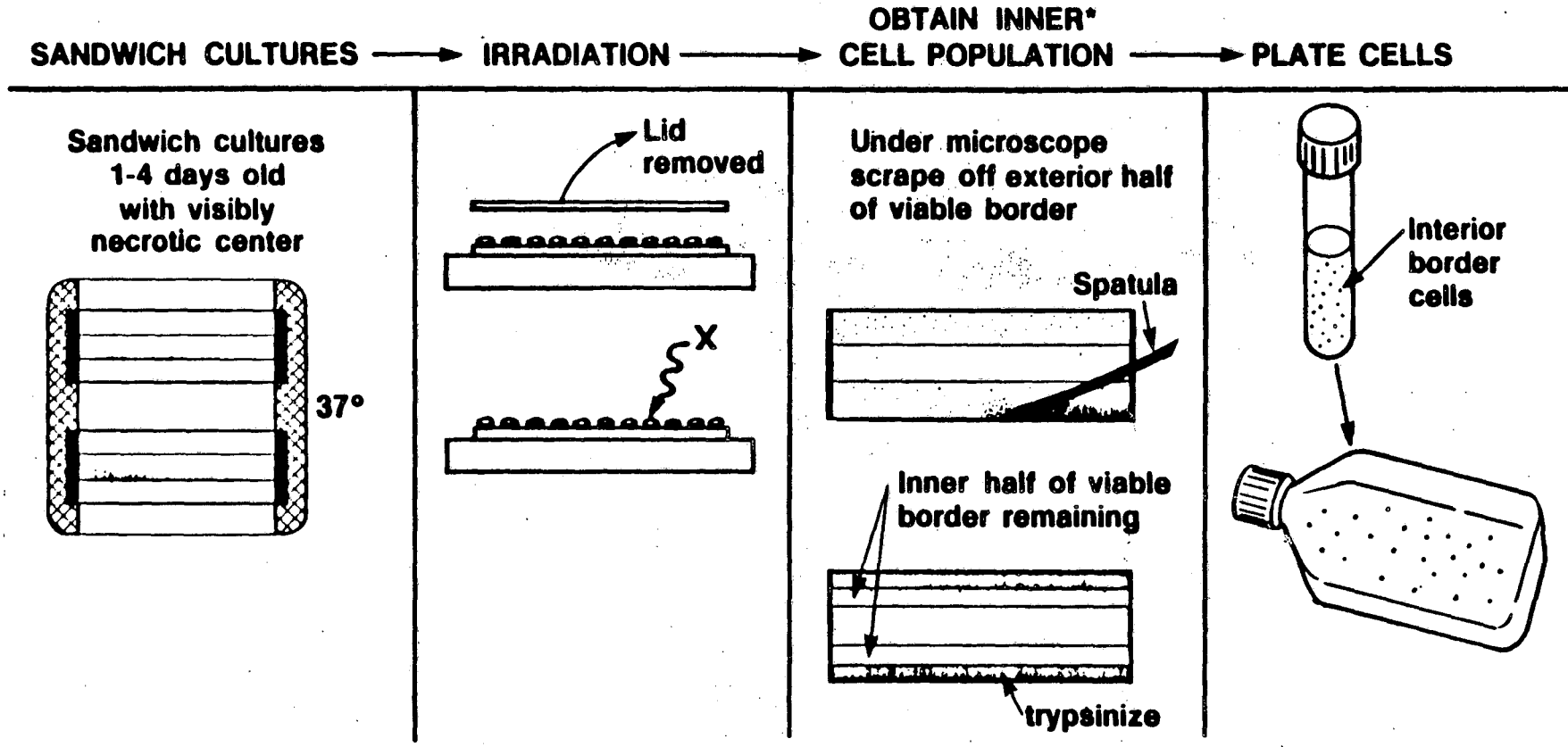

*Do analogous procedure for exterior border cells

Fig. 3

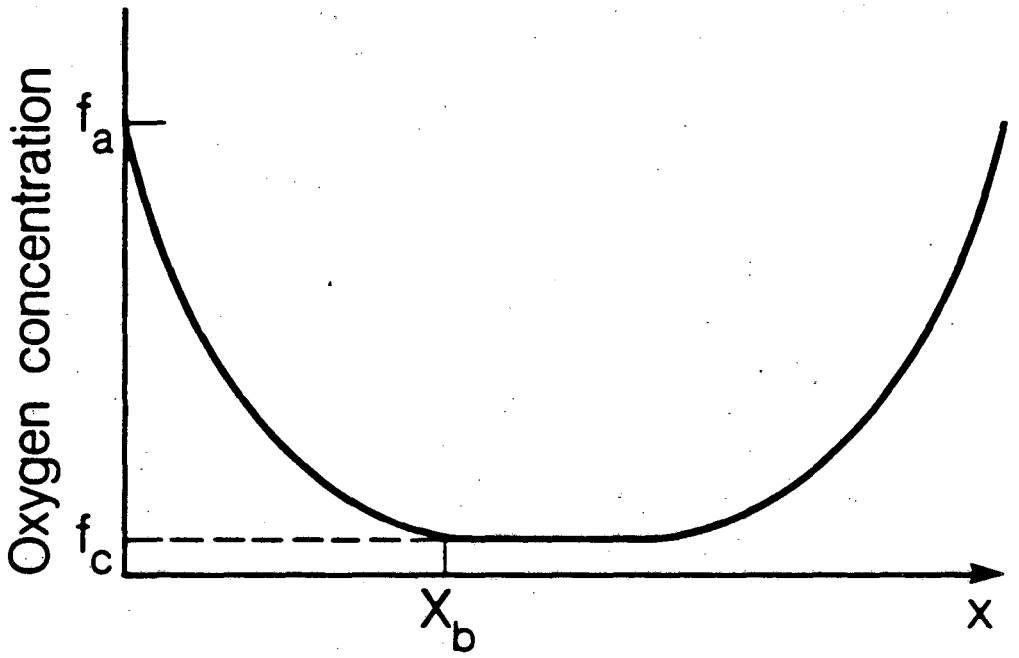

XBL 849-7978

Fig. 4

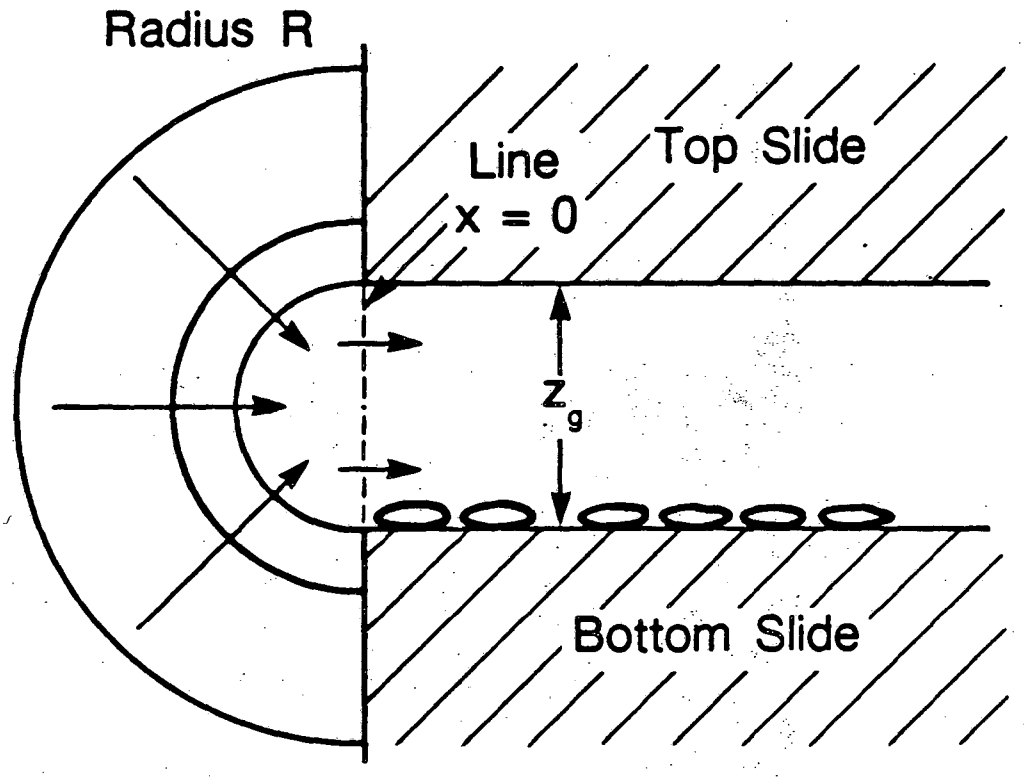

Fig. 5

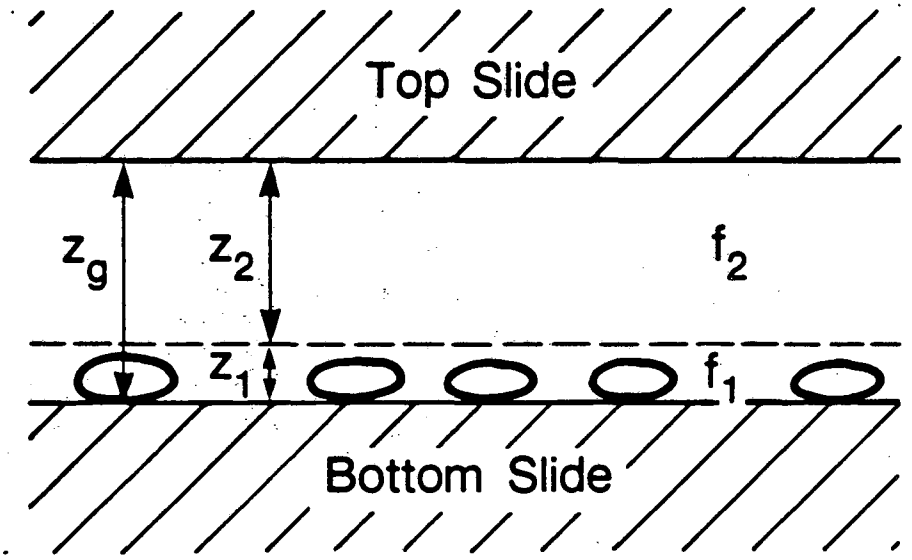

XBL 856-8365

Fig. 6

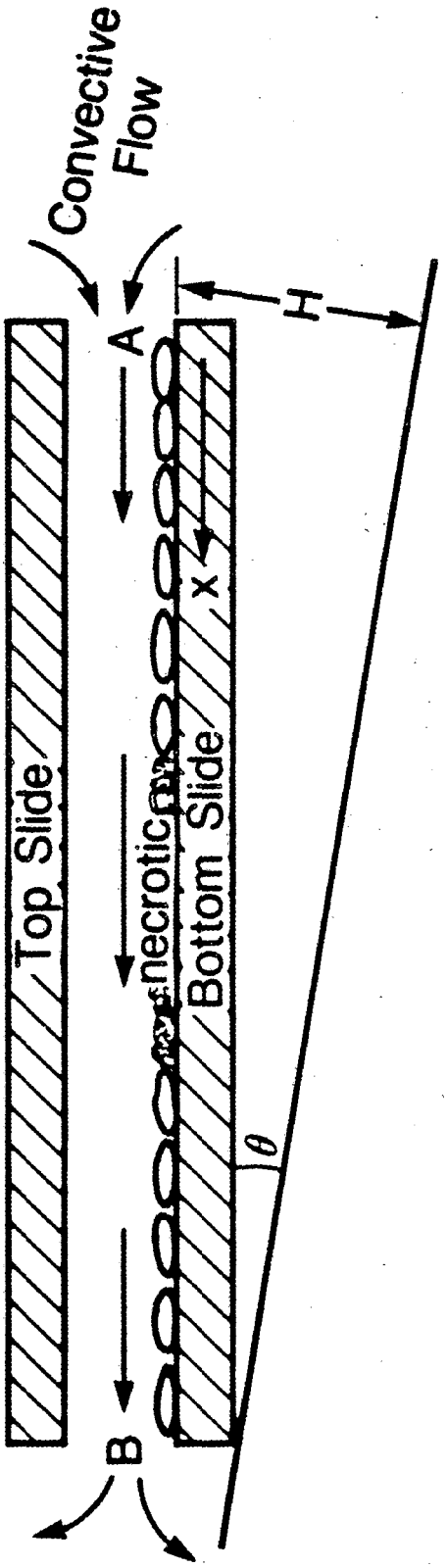
Convective
Flow
A
H
X
Top Slide
necrotic
Bottom Slide
θ
B
XBL 859-8491

Fig. 7

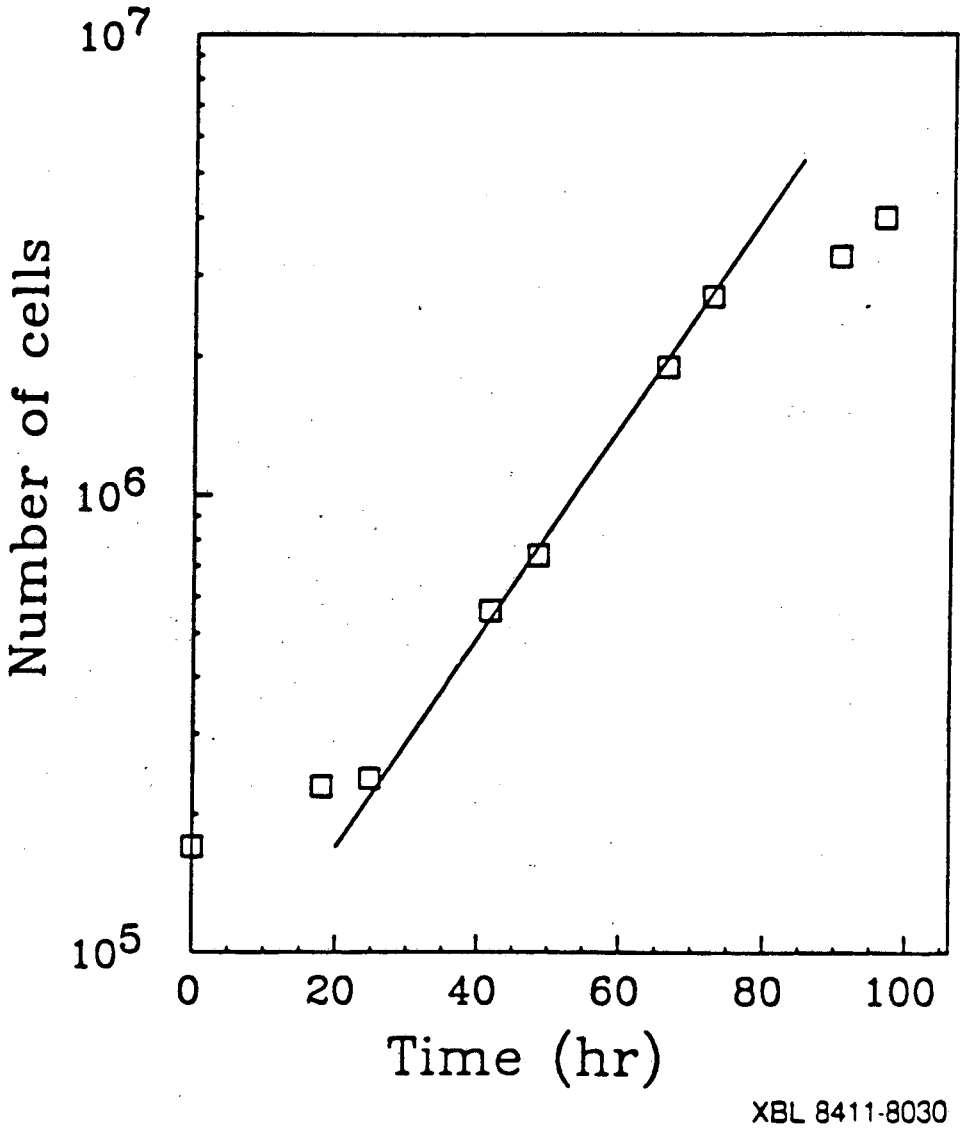
10^7
10^6
10^5
Number of cells
0
20
40
60
80
100
Time (hr)
XBL 8411-8030

Fig. 8

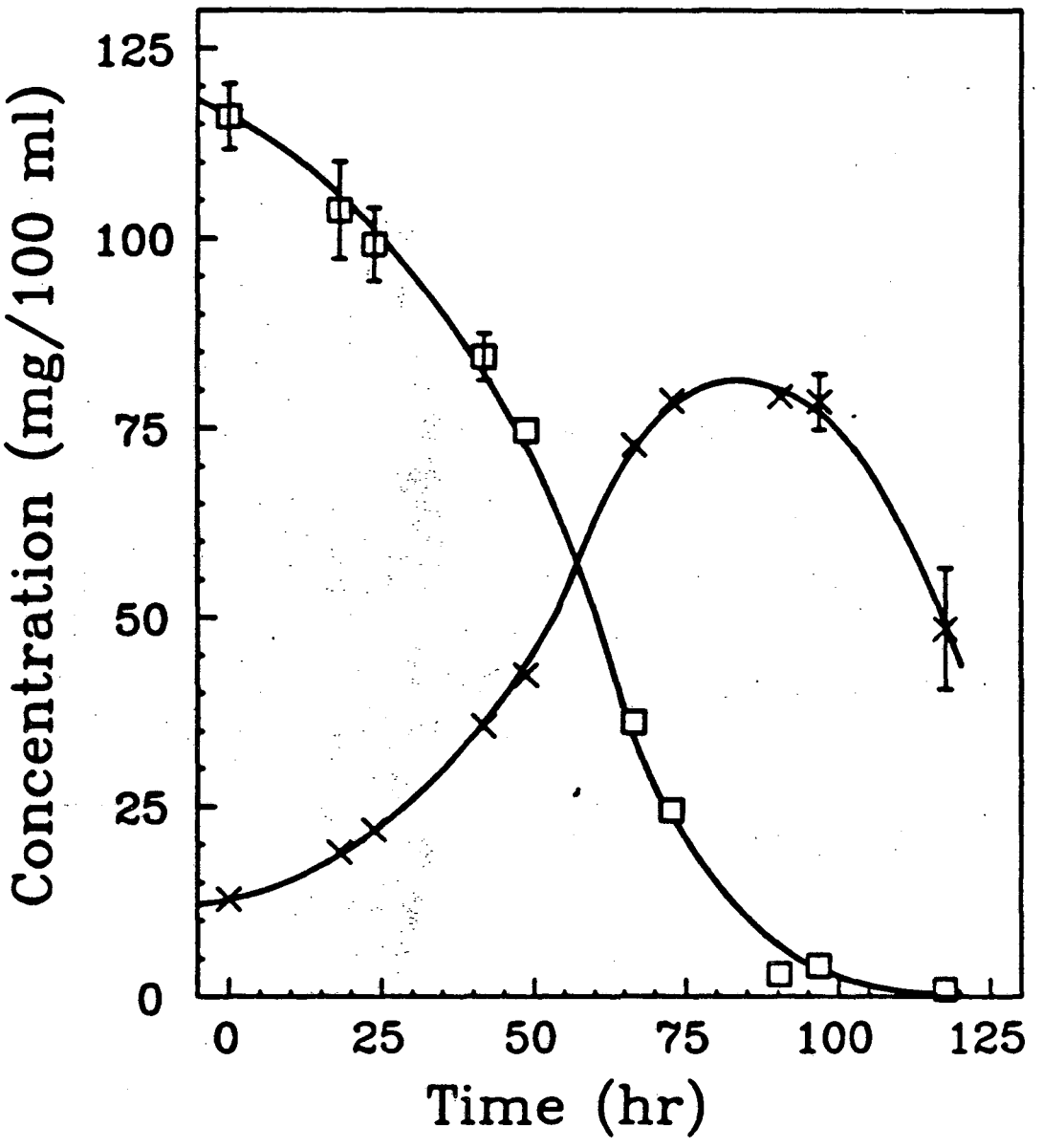
125
100
75
50
25
0
Concentration (mg/100 ml)
0
25
50
75
100
125
Time (hr)

Fig. 9

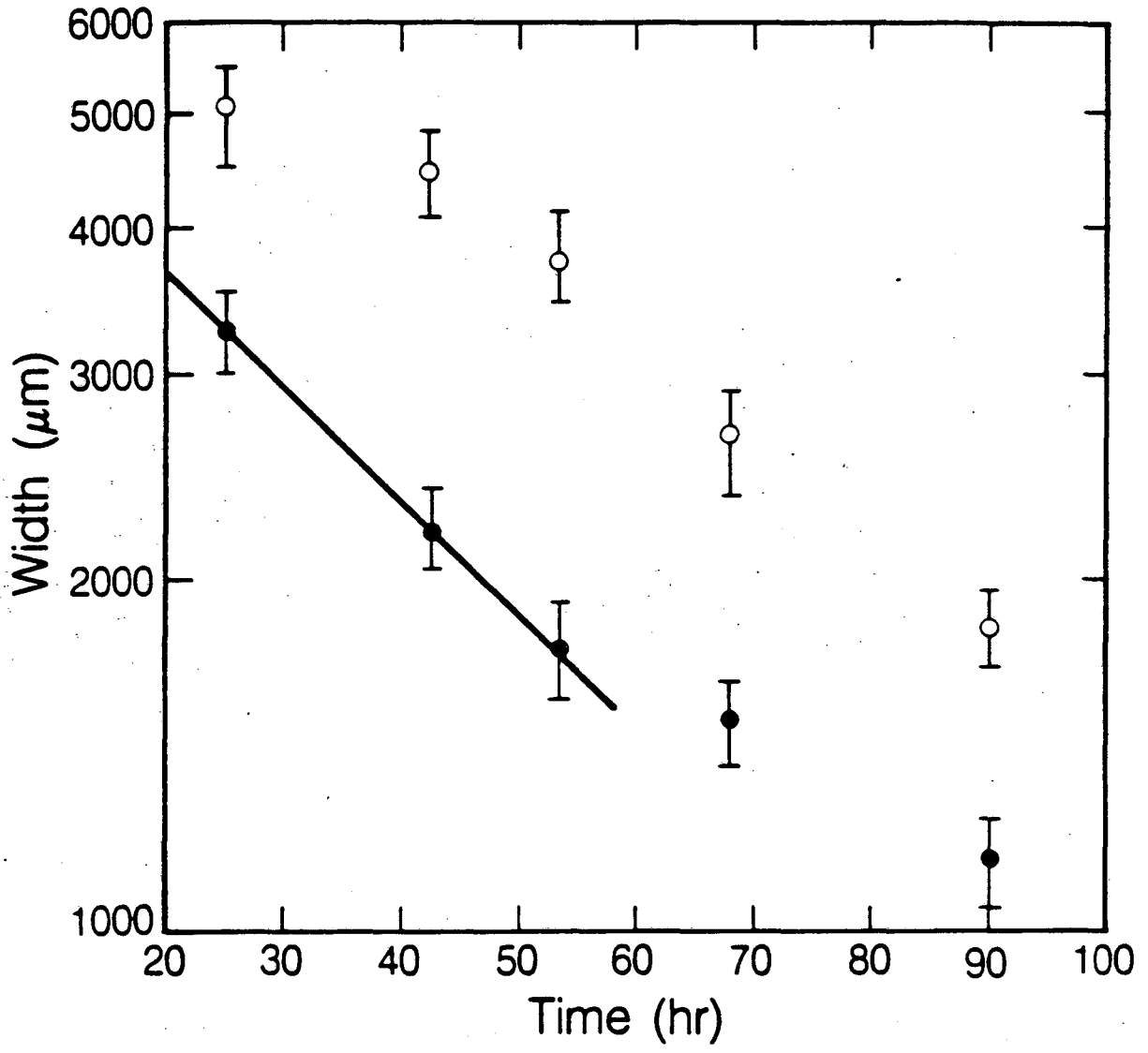

XBL 8411-8025

Fig. 10

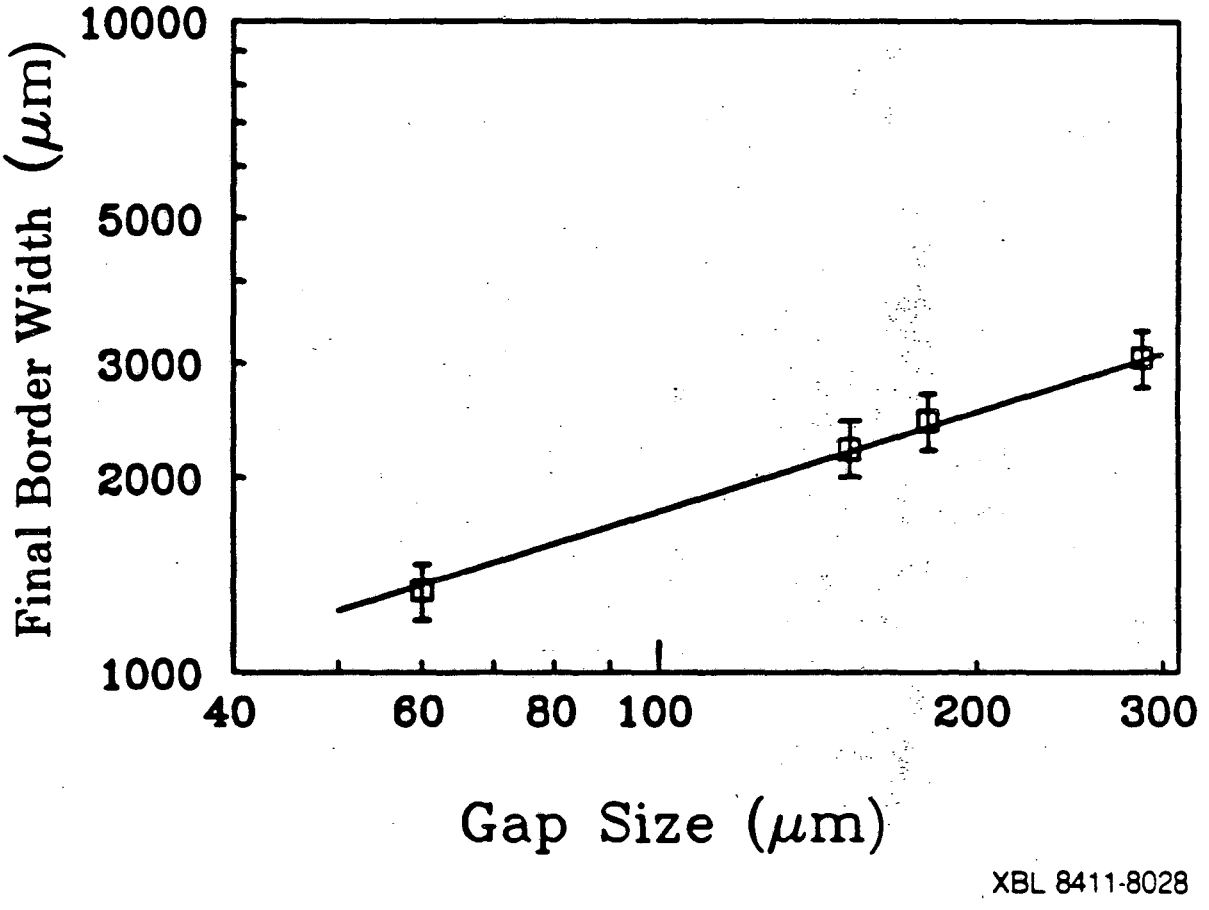
Final Border Width (μm)
10000
5000
3000
2000
1000
40
60
80
100
200
300
Gap Size (μm)
XBL 8411-8028

Fig. 11

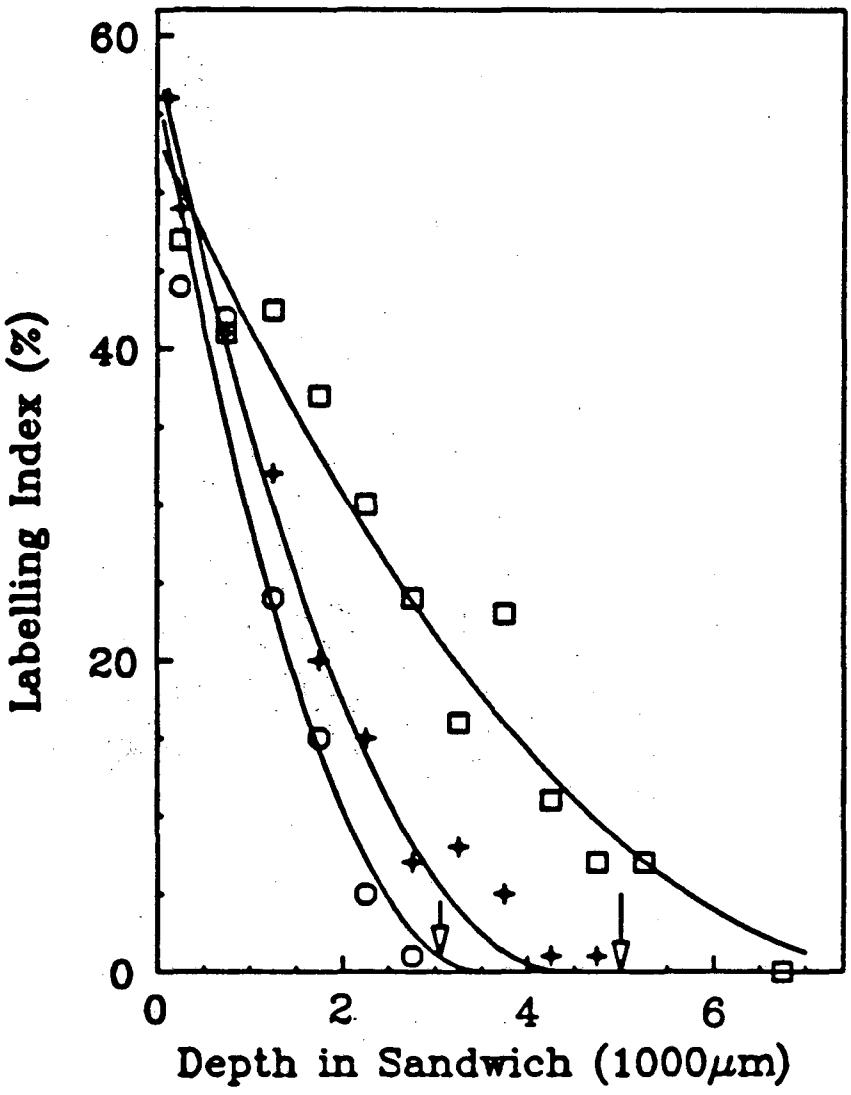

Fig. 12

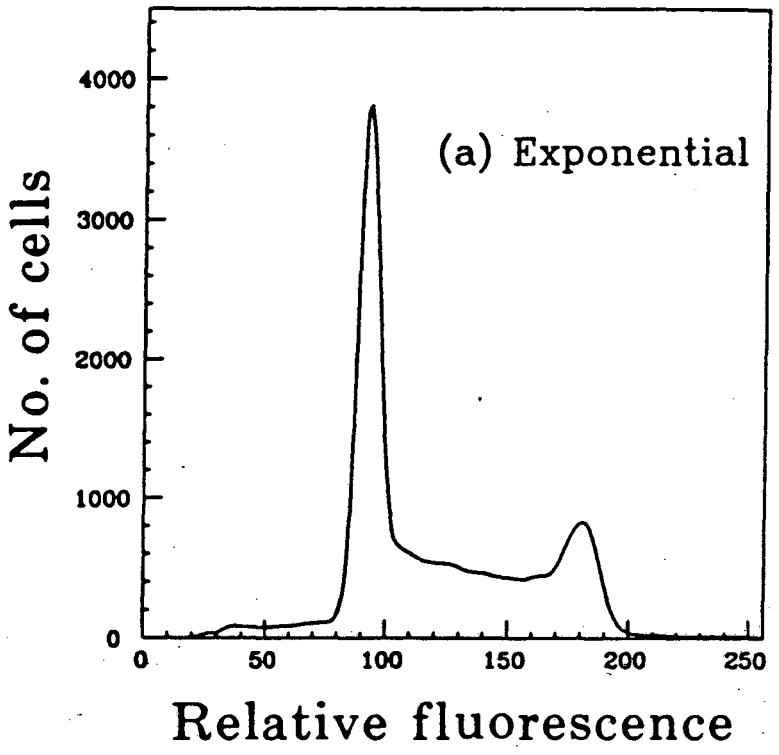
(a) Exponential
No. of cells
4000
3000
2000
1000
0
0
50
100
150
200
250
Relative fluorescence

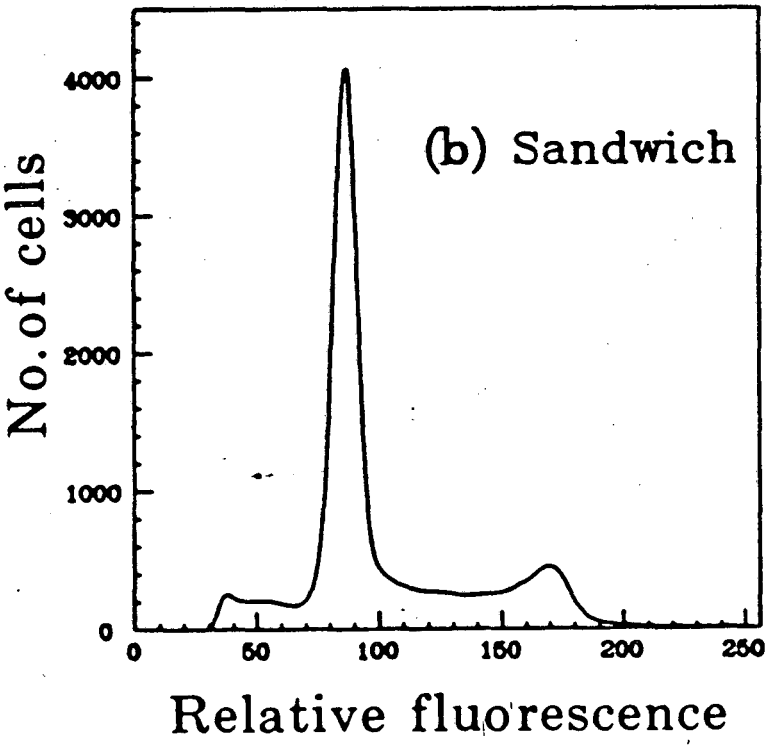
(b) Sandwich
No. of cells
4000
3000
2000
1000
0
0
50
100
150
200
250
Relative fluorescence

Fig. 13

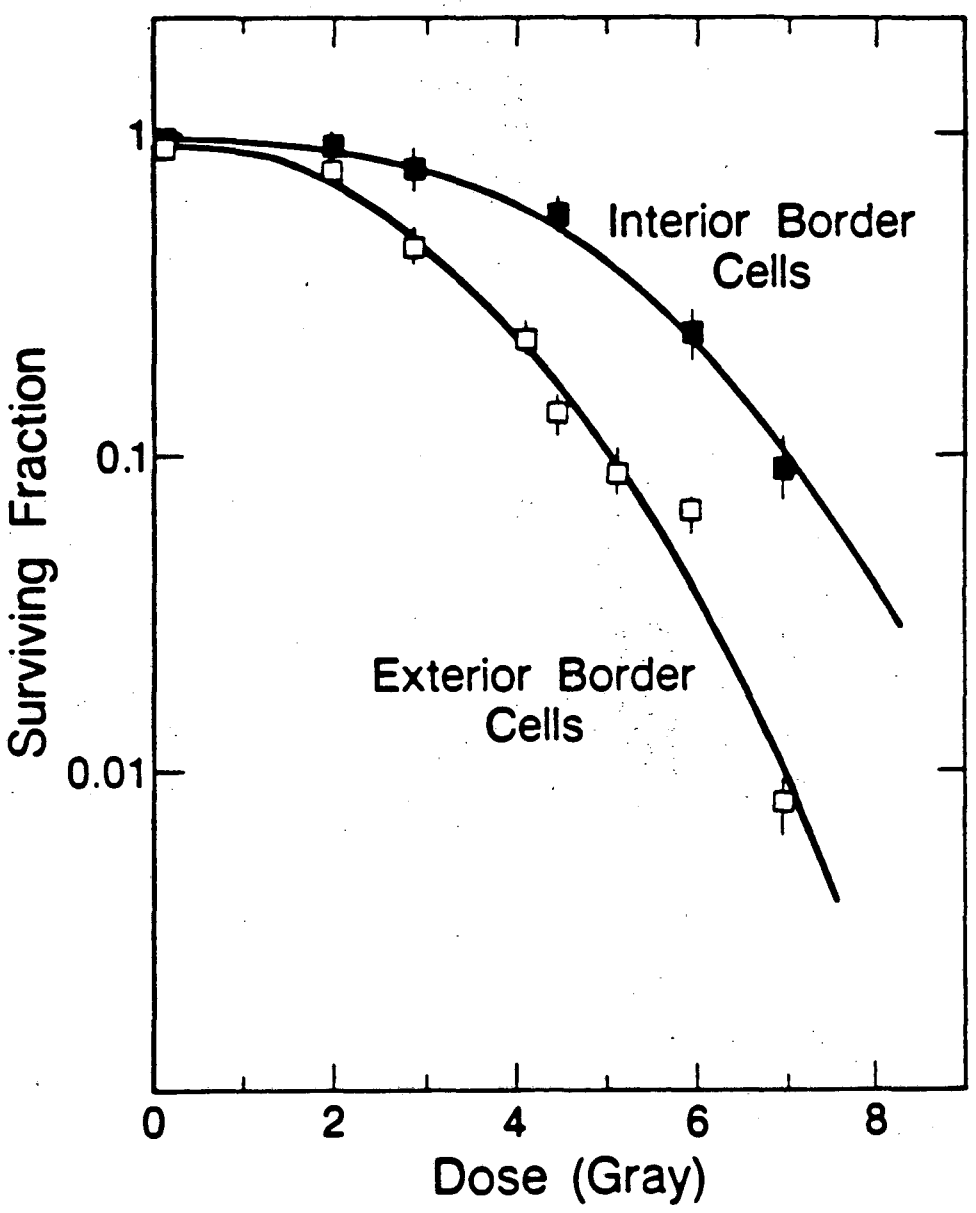
Surviving Fraction
1
0.1
0.01
0
2
4
6
8
Dose (Gray)
Interior Border Cells
Exterior Border Cells

Fig. 14

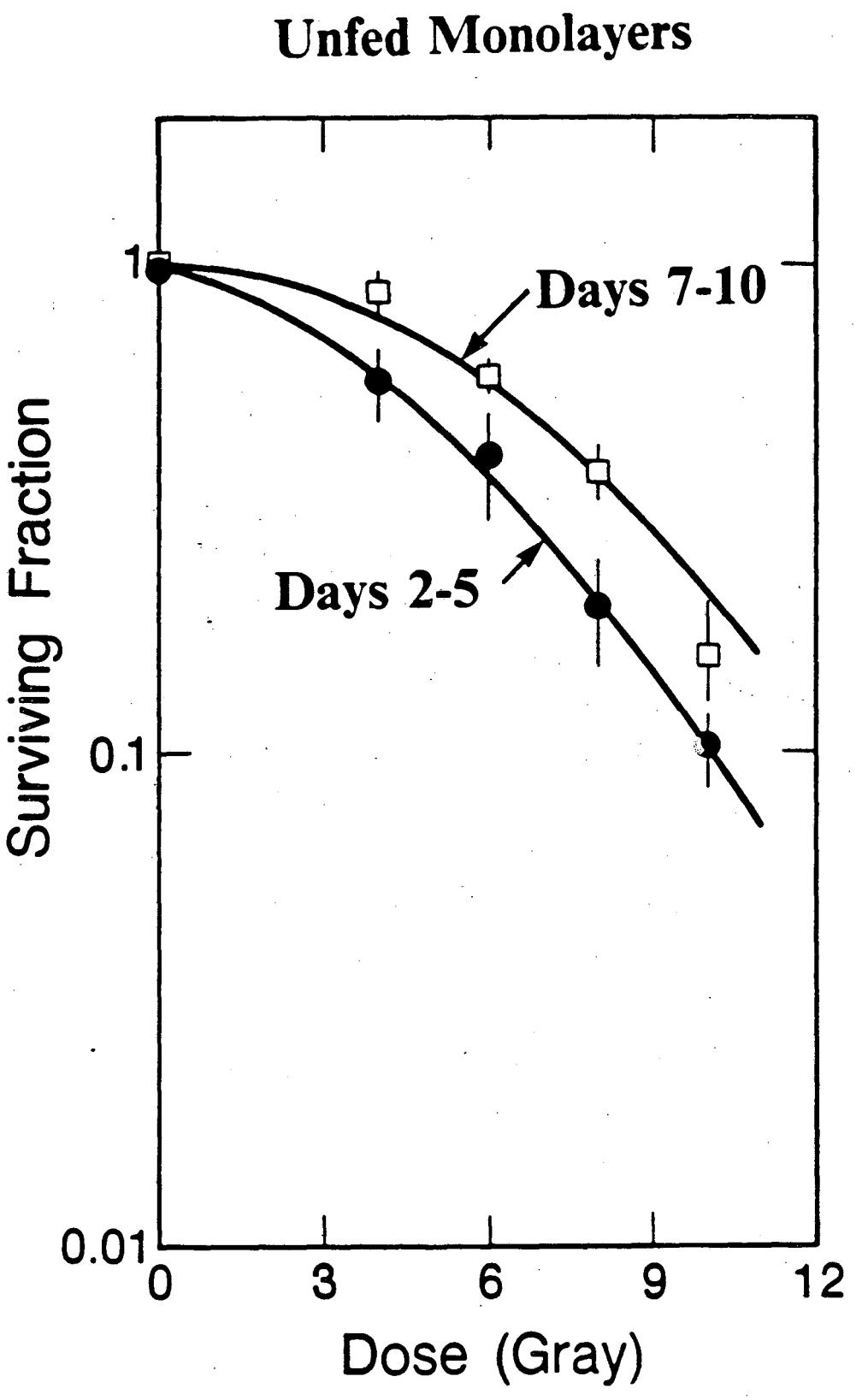
Unfed Monolayers
Days 7-10
Days 2-5
Surviving Fraction
1
0.1
0.01
0
3
6
9
12
Dose (Gray)

Fig. 15

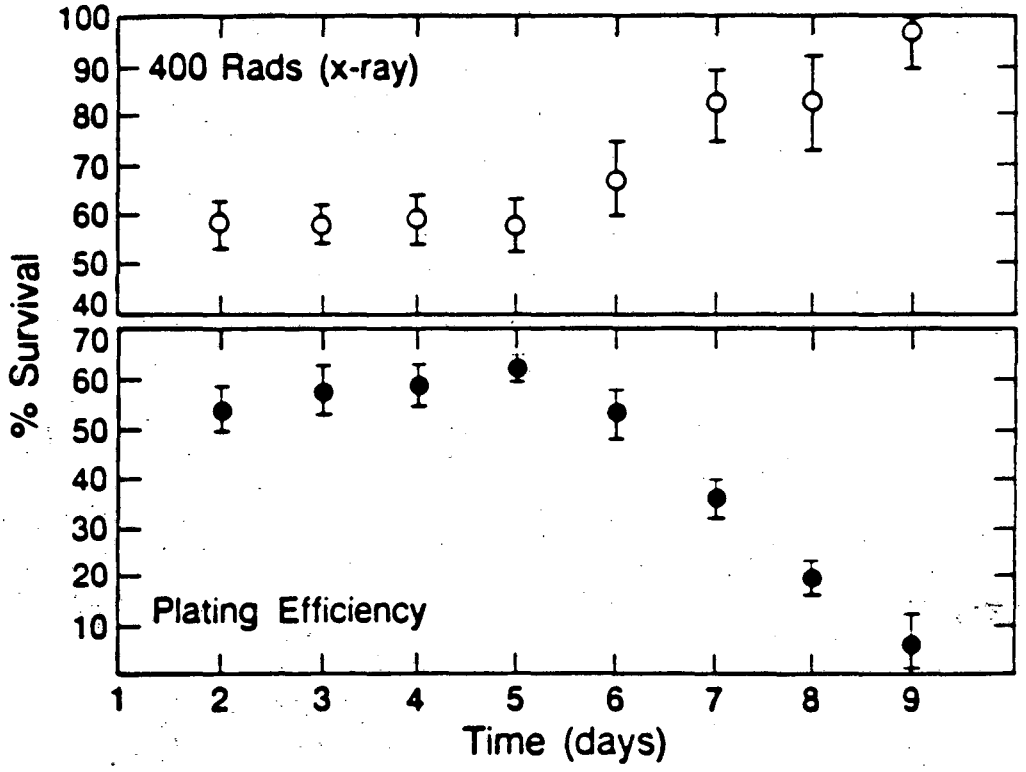
100
90
80
70
60
50
40
400 Rads (x-ray)
70
60
50
40
30
20
10
Plating Efficiency
% Survival
1
2
3
4
5
6
7
8
9
Time (days)

Fig. 16

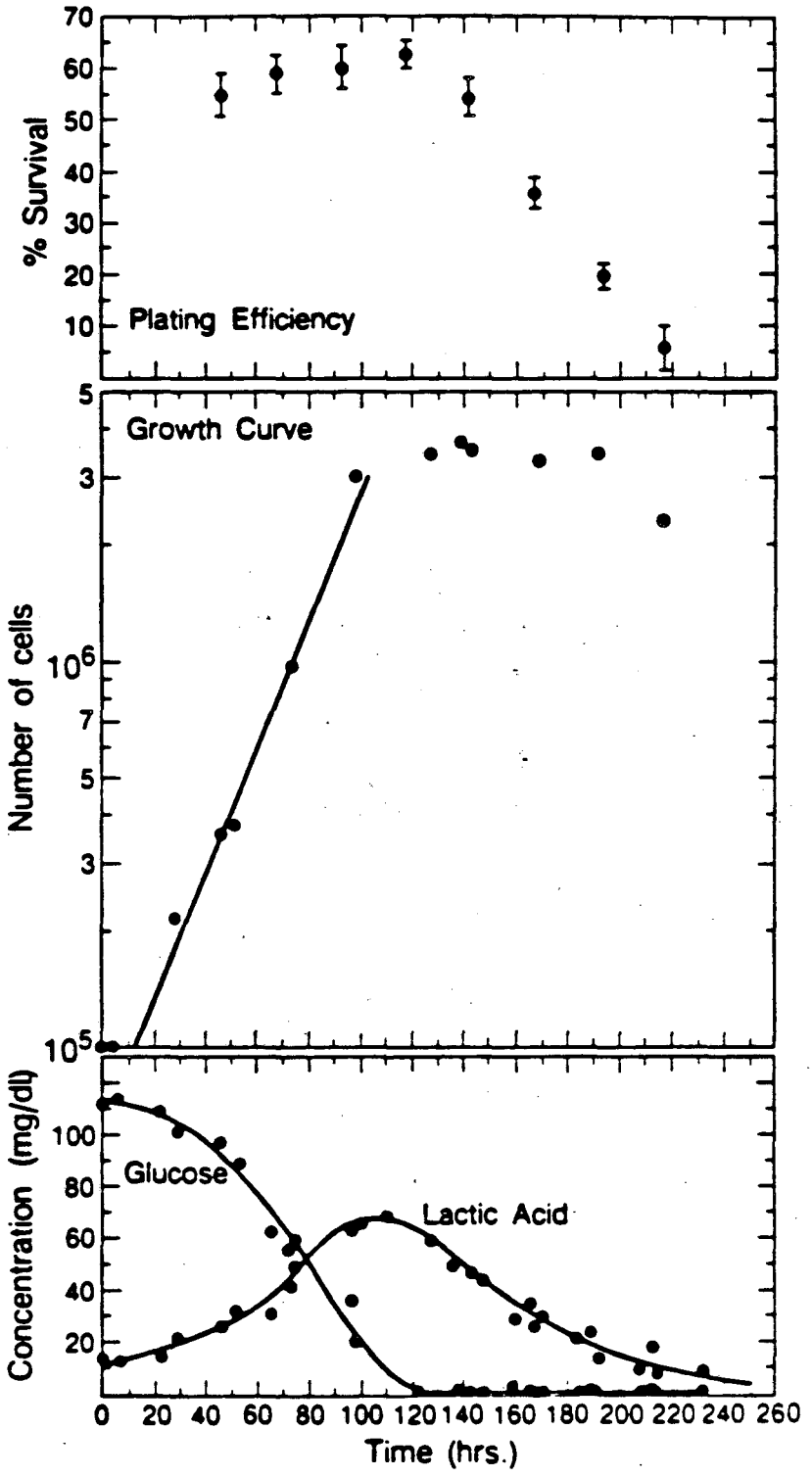
% Survival
Plating Efficiency
Growth Curve
Number of cells
Concentration (mg/dl)
Glucose
Lactic Acid
Time (hrs.)

Fig. 17

LAWRENCE BERKELEY LABORATORY
TECHNICAL INFORMATION DEPARTMENT
UNIVERSITY OF CALIFORNIA
BERKELEY, CALIFORNIA 94720